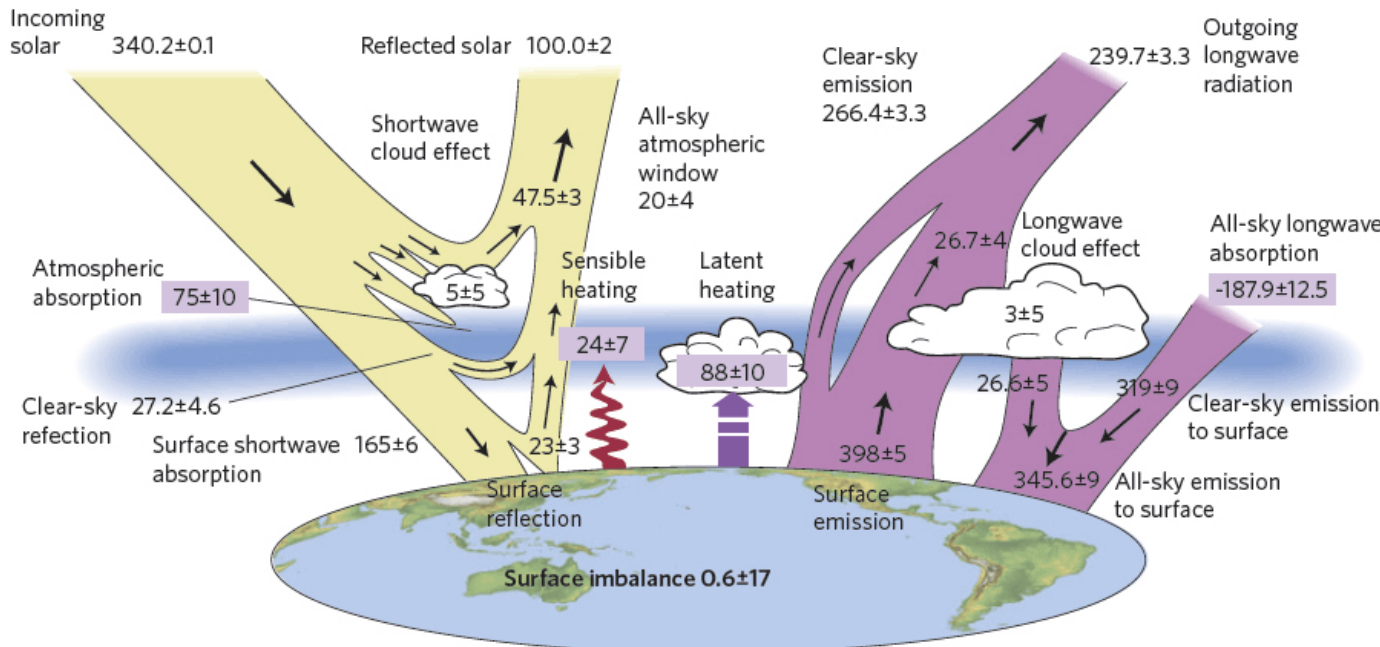


Cloud Radiative Effect Evaluation using CC4CL Broadband Flux Algorithm

M. Christensen^{1,2}, W. Jones¹, C. Poulsen¹, G. McGarragh², G. Thomas¹, R. Grainger²
¹RAL Space, ²Oxford,

Global Radiation Budget

- Clouds globally cool the planet by -17 W m^{-2} (Loeb et al., 2009).
 - *cooling* in the shortwave is $-47.5 \pm 3.0 \text{ W m}^{-2}$
 - *warming* in the longwave is $+26.7 \pm 4.0 \text{ W m}^{-2}$
- Radiative impact from anthropogenic CO₂ since 1750 is $2.63 \pm 0.26 \text{ W m}^{-2}$
- Uncertainties in the representation of clouds can have a considerable impact on the simulated climate.



Stephens et al. 2012, *Nat. GeoSci.*



CC4CL

(Community Code 4 CLimate)



- Algorithm used in the ESA CCI (Climate Change Initiative)

■ Aerosol-ORAC

- Optimal estimation algorithm
- Similar forward model to cloud retrieval
- Dual view algorithm
- Visible channels only
- NN cloud mask
- 10km product
- Thomas et al. 2010

• Cloud-CC4CL

- Optimal estimation algorithm
- Similar forward model to aerosol
- Single view algorithm
- Visible and IR
- NN cloud mask
- 1km retrievals
- Poulsen et al 2012

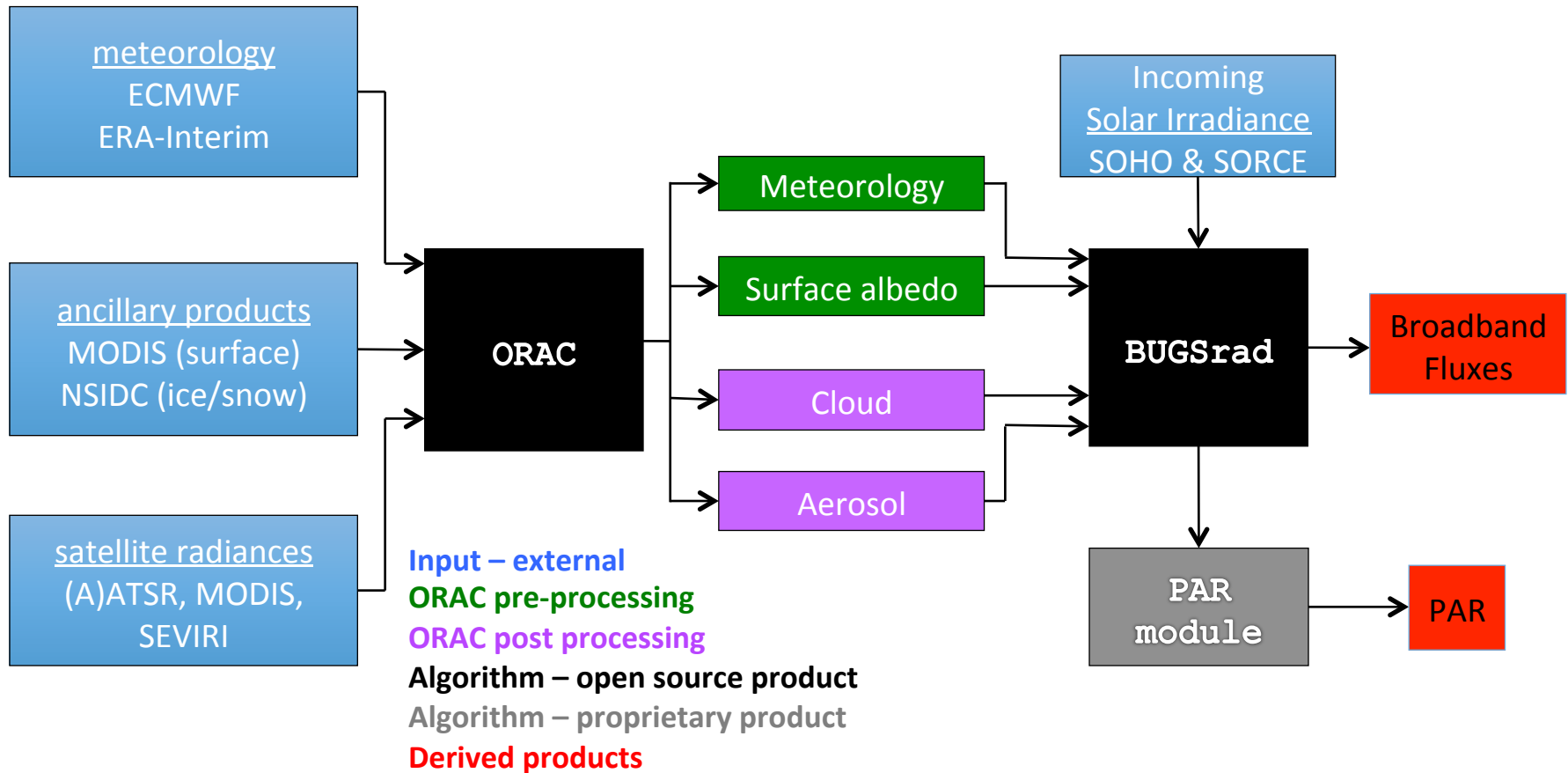
Retrieved Quantities

Variable	Aerosol CCI	Cloud CCI
Resolution	10km	1km
Time period	1995-2012	1995-2012
Aerosol Optical depth	x	
Aerosol effective radius	x	
Angstrom	x	
Cloud optical depth		x
Cloud effective radius		x
Cloud top height/pressure/ temperature		x
Cloud ice/water path		x
Cloud mask		x
Cloud phase and type		x
Cloud spectral albedo		x
Top and bottom longwave and shortwave radiative flux	x	x
Corrected cloud top height		x

Optimal Retrieval of Aerosol and Cloud (ORAC): Broadband Fluxes

ORAC is part of CC4CL (Community Code for CLimate) and applied to many satellite sensors.

- AVHRR, ATSR-2, AATSR, SEVIRI, & MODIS



Waveband	primary absorber
200 – 689 nm	O ₃
689 – 1299 nm	H ₂ O
1299 – 1905 nm	H ₂ O
1299 – 2500 nm	H ₂ O
2500 – 3509 nm	H ₂ O
3509 – 4000 nm	H ₂ O
Longwave	
4.5 – 5.2 μm	H ₂ O
5.2 – 5.8 μm	H ₂ O
5.8 – 7.1 μm	H ₂ O
7.1 – 8.0 μm	H ₂ O, CH ₄ , N ₂ O
8.0 – 9.1 μm	H ₂ O, CH ₄ , N ₂ O
9.1 – 10.2 μm	O ₃ , H ₂ O
10.2 – 12.5 μm	H ₂ O
12.5 – 14.9 μm	H ₂ O, CO ₂
14.9 – 18.5 μm	H ₂ O, CO ₂
18.5 – 25 μm	H ₂ O
25 – 36 μm	H ₂ O
36 – ∞	H ₂ O

BUGSrad

Radiative Flux Algorithm

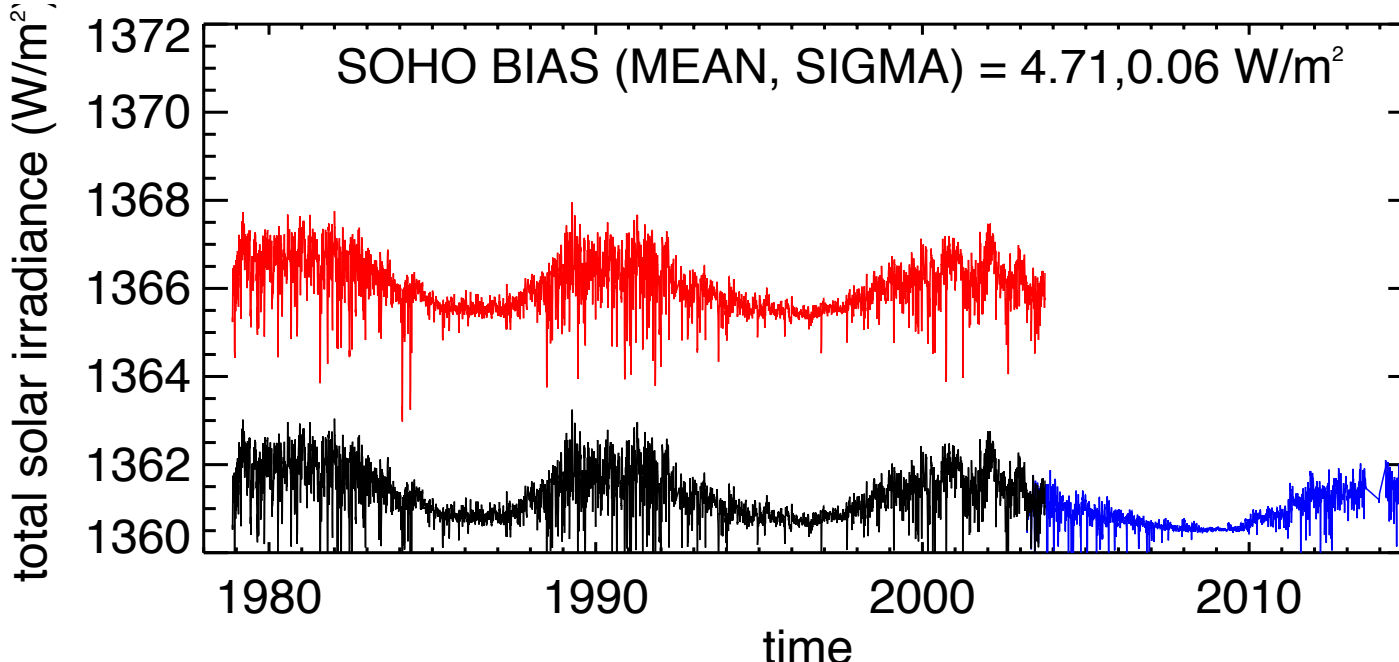
- Correlated-k distribution method.
 - ❖ based on Fu Liou (1992)
- Two-stream approximation.
- Plane-parallel cloud approximation.
- Developed for the Community Atmosphere Model (CAM) [Collens et al., 2004].
- Used to generate radiative fluxes and heating rate profiles using CloudSat observations.
- Excellent agreement between CloudSat/MODIS and CERES (Hendersen et al. 2013).
- Open source:
<http://biocycle.atmos.colostate.edu/shiny/BUGSrad/>

Output

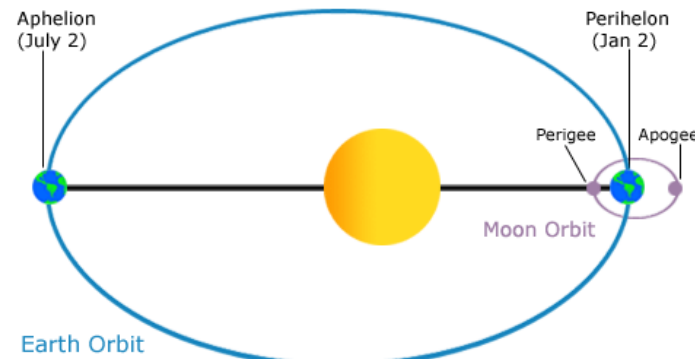
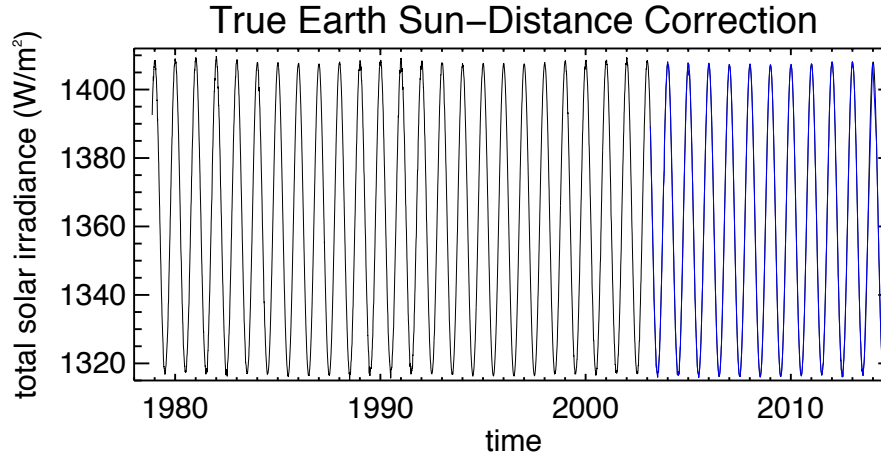
- **Top** and **bottom** of atmosphere longwave and shortwave fluxes.
 - ❖ Observed: With cloud and aerosol properties
 - ❖ CLEAR: Assuming no cloud and aerosol properties
- Diffuse and direct surface shortwave radiative fluxes
- Photosynthetic Active Radiation (PAR)

Fu-Liou model option is available for intercomparison.
 More accurate with more SW bands but 3 times slower.

Total Solar Irradiance



- SoHO and SORCE TSI observations are used to characterize top of atmosphere incoming shortwave radiative flux.
- Uncertainty estimates using this data $1361 \pm 0.8 \text{ W/m}^2$ (Loeb et al. 2008).

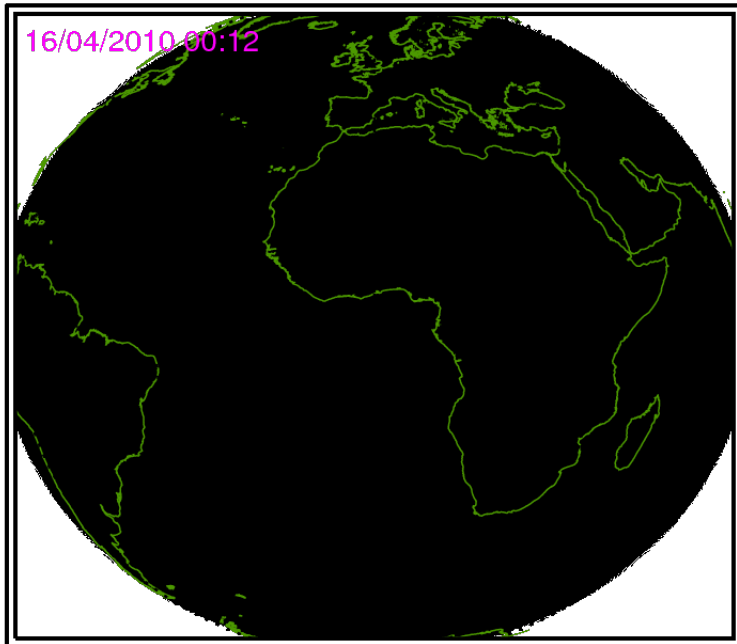


$$S_{fac}(t) = 1.0001 + 0.0334\cos(t) + 0.00128\sin(t) + 0.00071\cos(2t) + 0.000077\sin(2t)$$

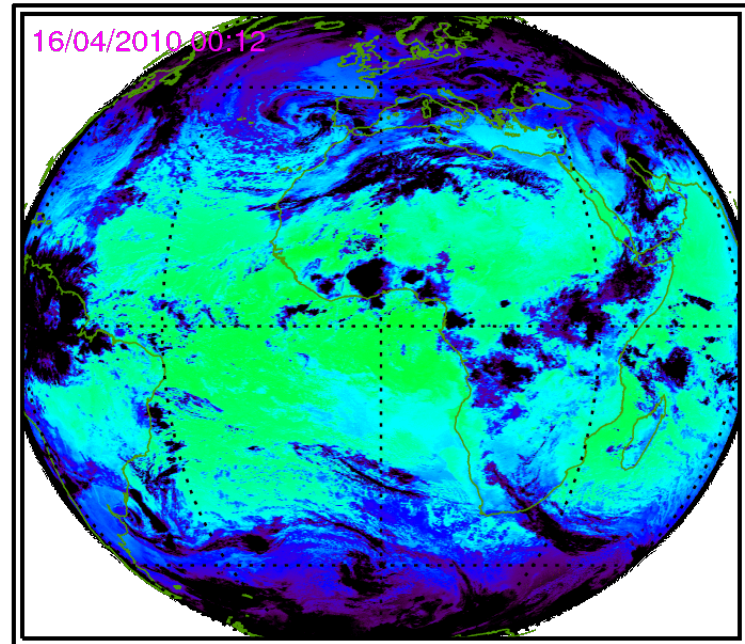
Image from NOAA

Application to SEVIRI Observations

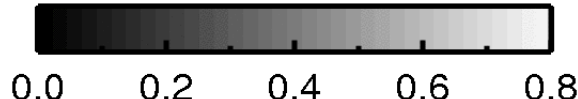
0.55- μm Reflectance (ch 2)



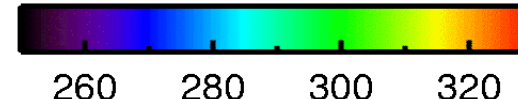
3.9- μm Brightness Temperature (ch 4)



$R_{\text{CH}2}$

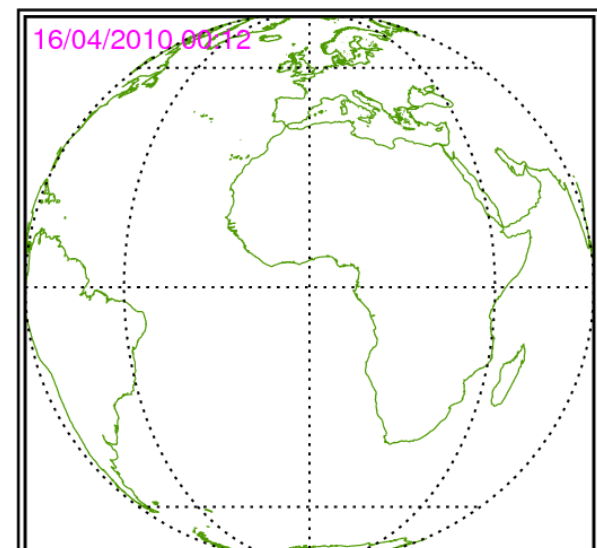


$T_b \text{ CH}_4 \text{ (K)}$

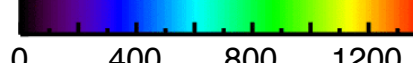


Application to SEVIRI Observations

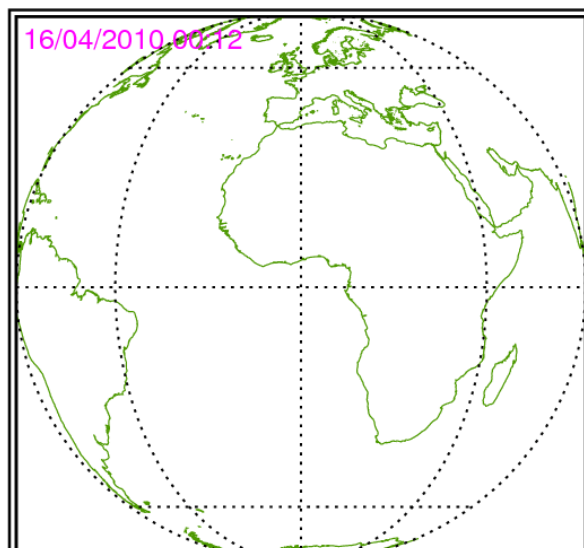
TOA incoming shortwave flux



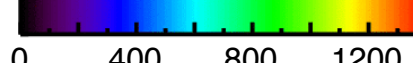
TOA LWUP (W/m²)



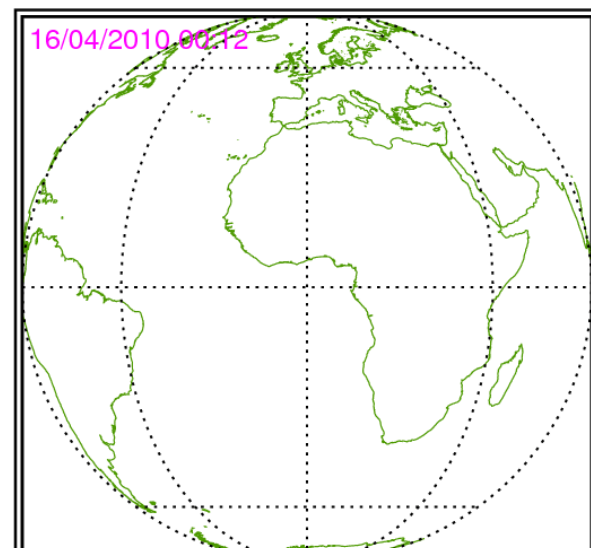
TOA outgoing shortwave flux



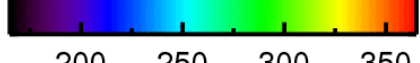
TOA SWDN (W/m²)



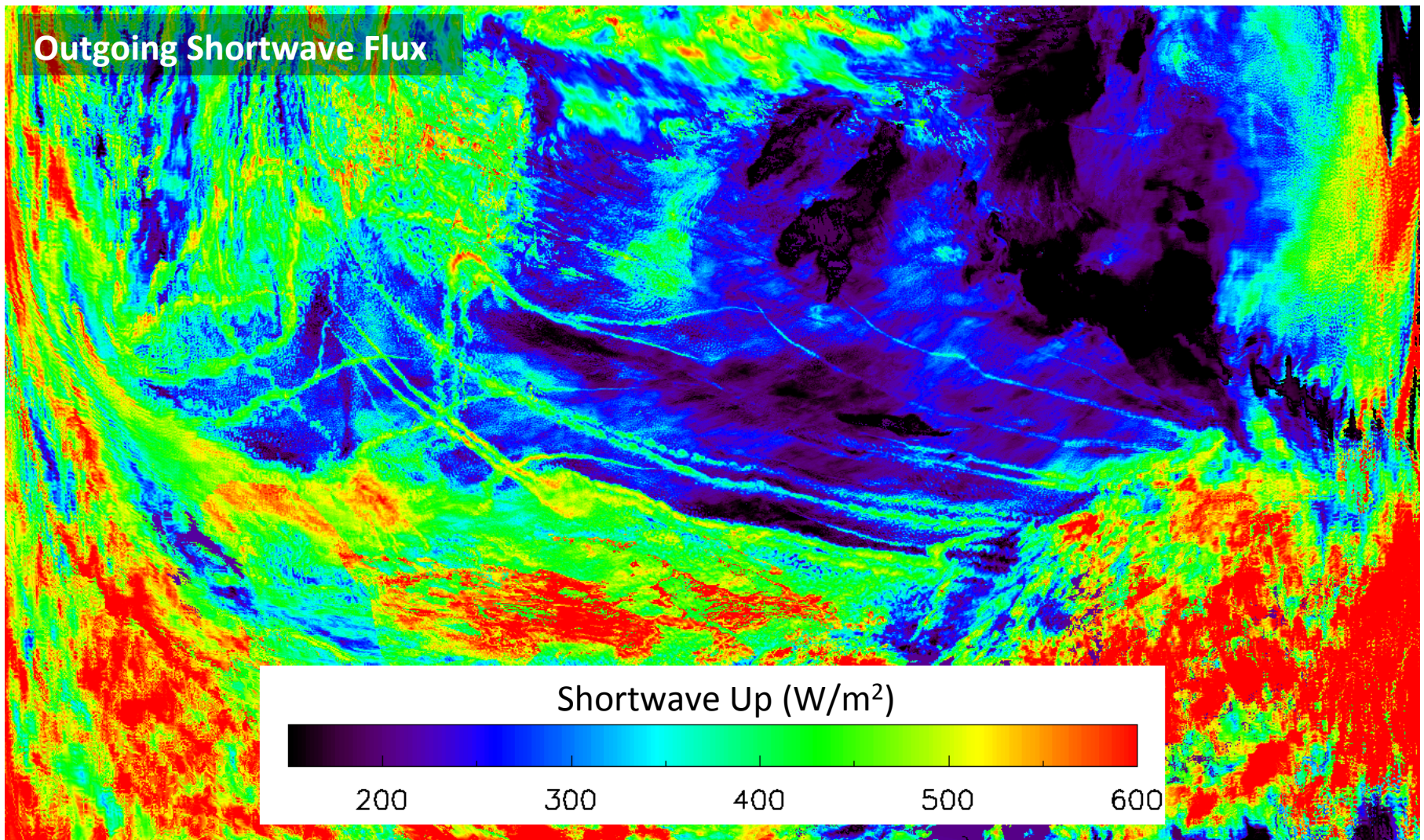
TOA outgoing longwave flux



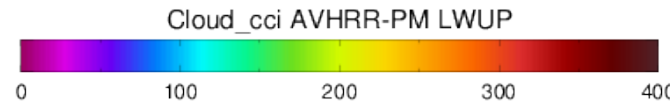
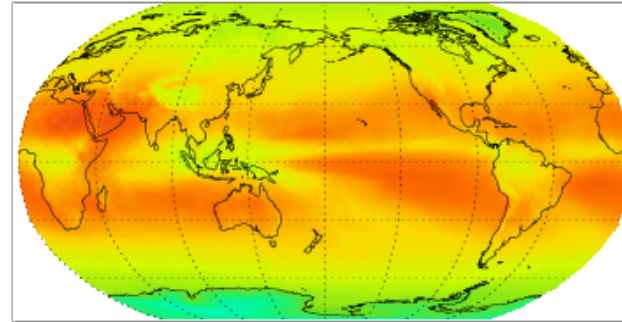
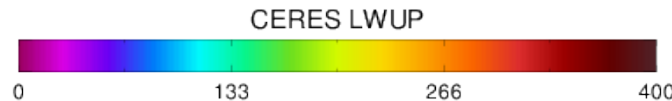
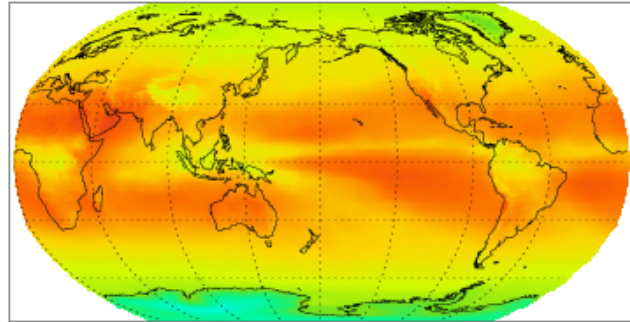
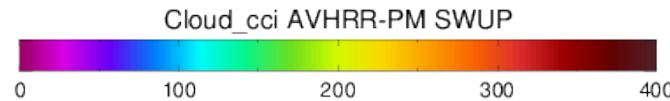
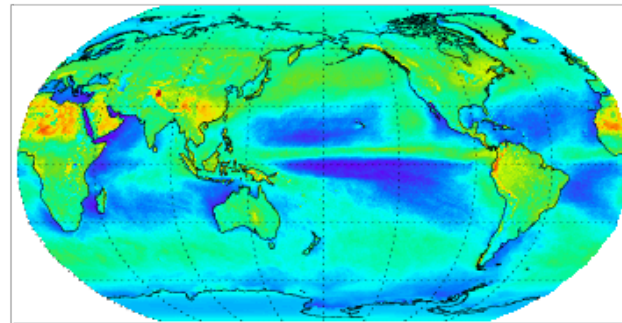
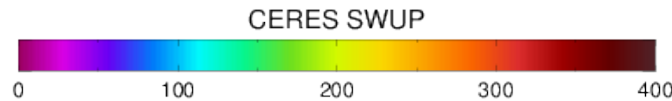
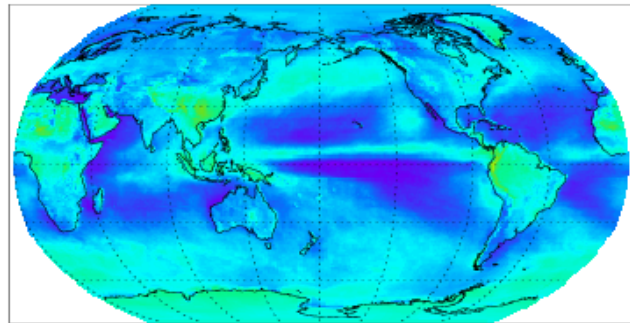
TOA LWUP (W/m²)



Ship Tracks – ORAC applied to MODIS



Application to AVHRR Observations



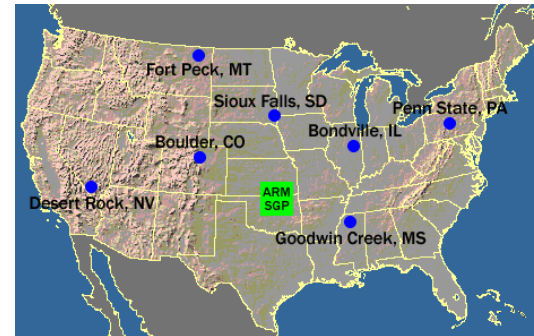
- CCI plans to process whole time-series 1982 – present.

Figures courtesy of Martin Stengle, DWD.

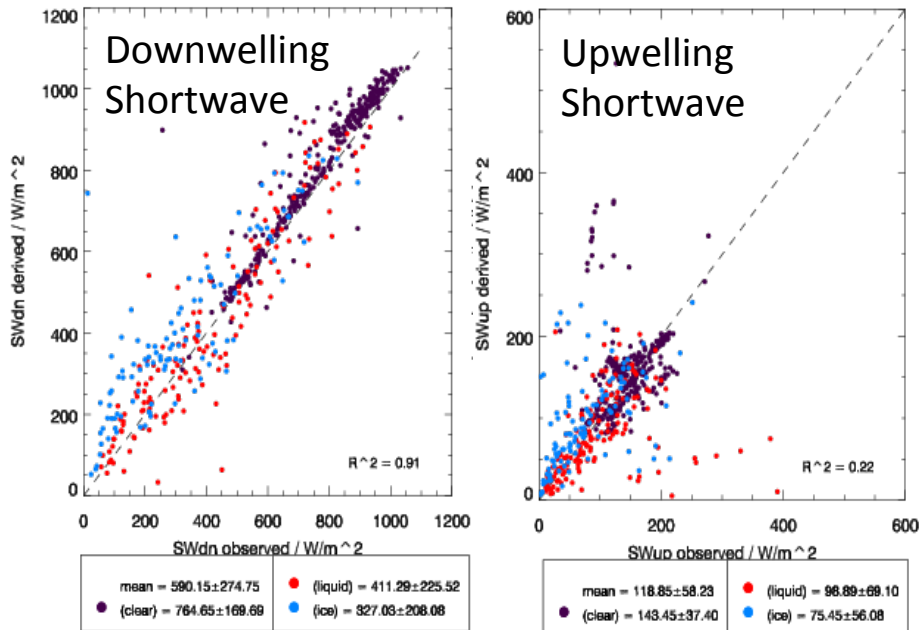
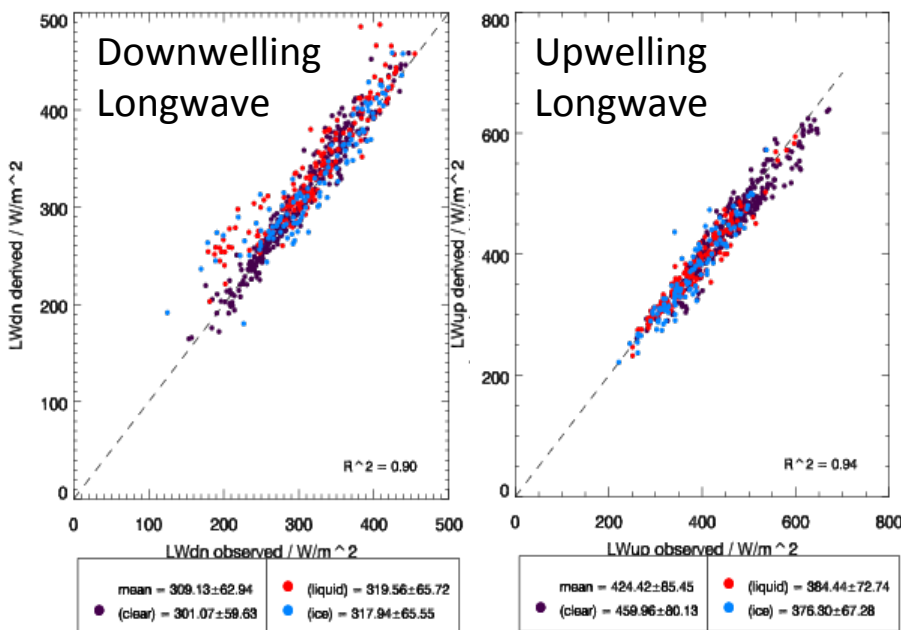
AVHRR annual mean: 2008

Ground-Based Validation

- Data: ORAC-MODIS & SURFRAD (ground sites)
- Period: 4-months (January, April, October) in 2008
- SURFRAD overpasses 727



Surface Fluxes – SURFRAD Validation

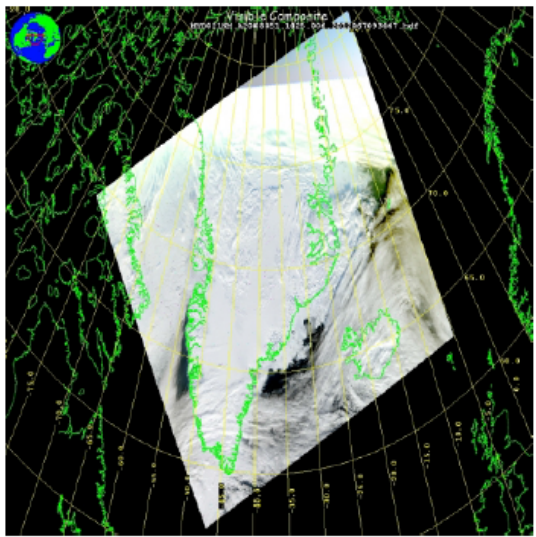


Relative biases

- Net Longwave ~ 1%
- Net Shortwave = 5%

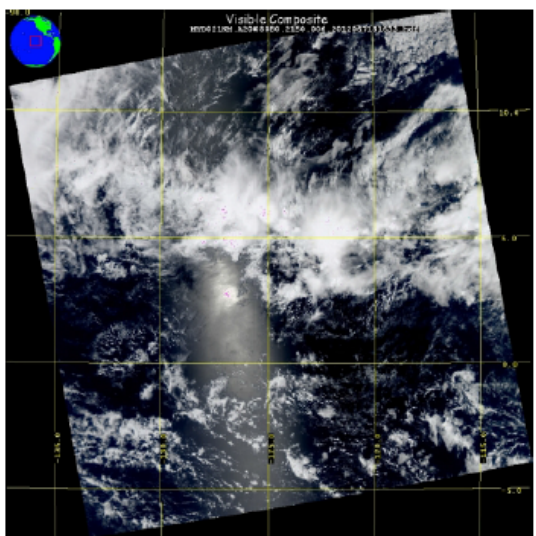
CERES Comparison

Test Scenes



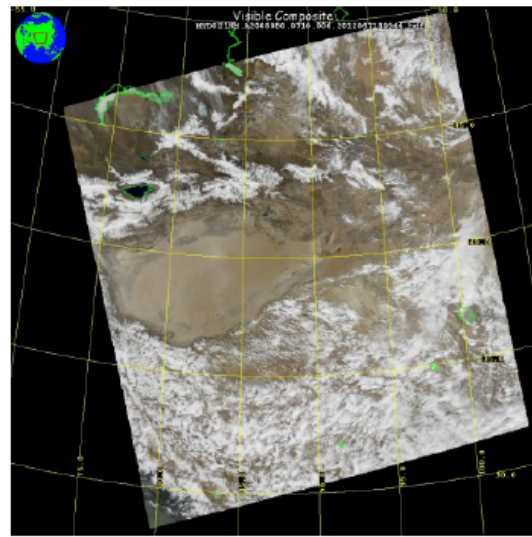
02/20/2008
14:25 UTC

Greenland



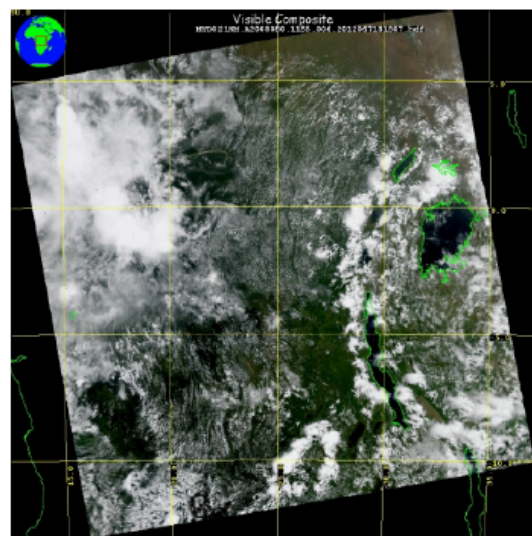
03/20/2008
21:50 UTC

North
Atlantic



03/20/2008
07:10 UTC

Taklamakan
desert



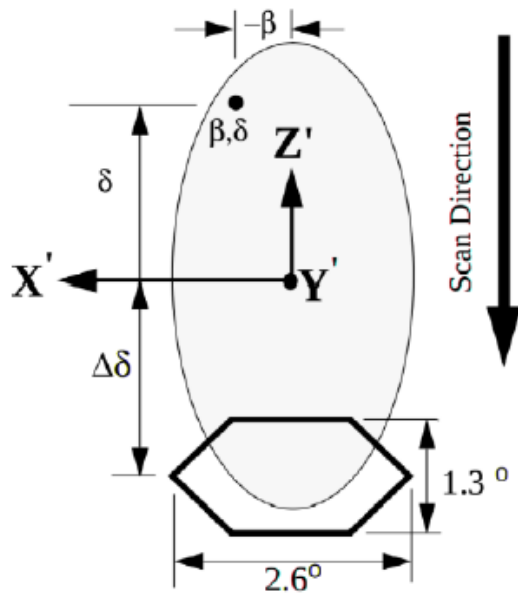
02/20/2008
11:55 UTC

Central
Africa

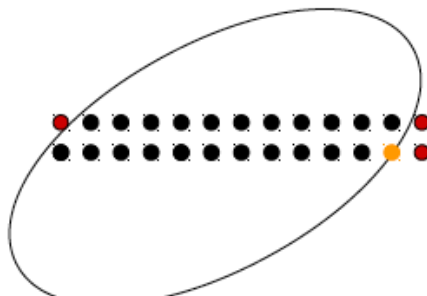


Collocation

CERES footprint

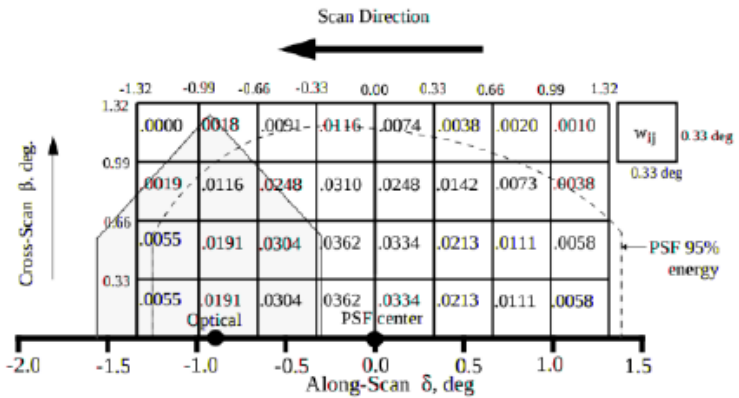


Collocation according to CERES: ATBD Subsystem 4.4 - Convolution



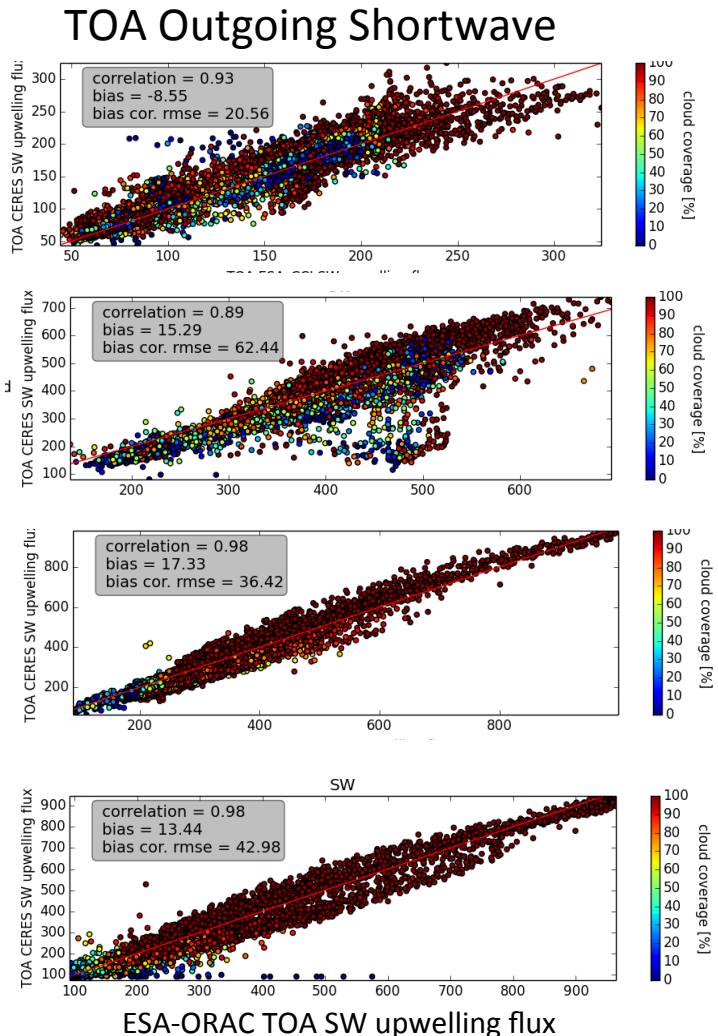
● – MODIS pixel

- Retrieve β_{img} , δ_{img} for each imager pixel
- Compare PSF: $P_{\text{img}} \geq \text{PSF}_{95\%}$
- Average imager pixel over footprint including PSF weights

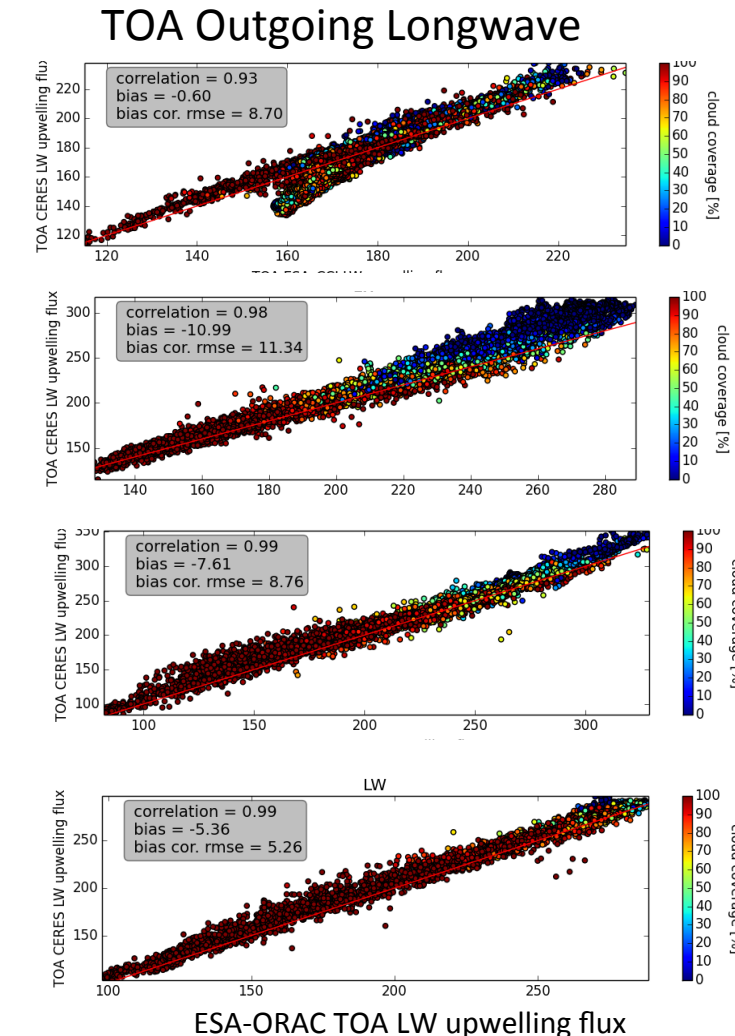


CERES Comparison

Greenland



Taklamakan
Desert



Central Africa

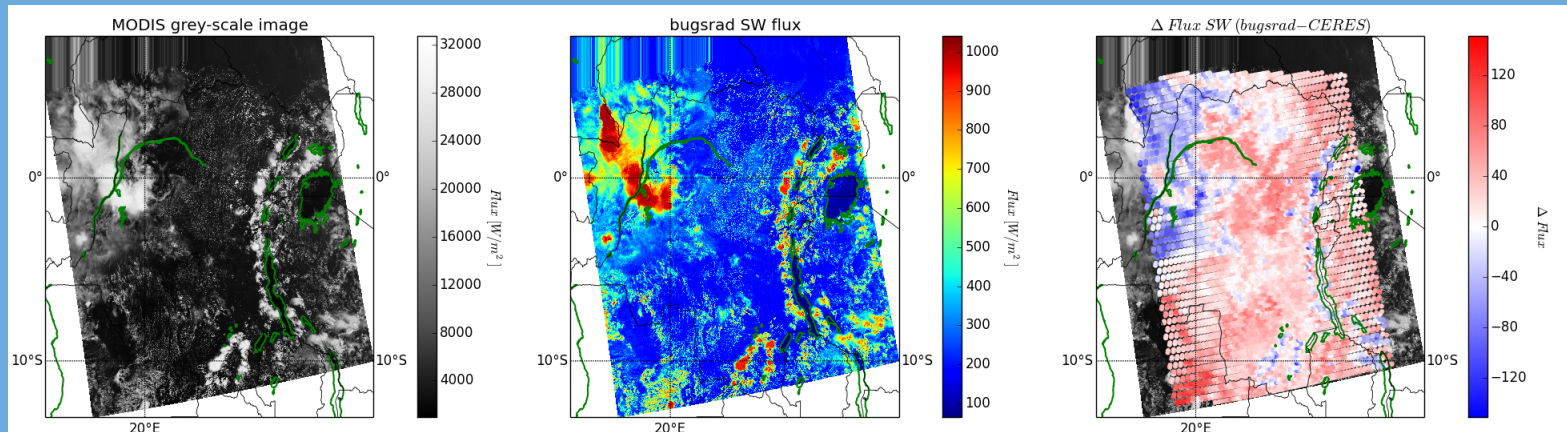
North Atlantic

- Correlations are high and tend to be above 0.95.
- Still room to improve shortwave and longwave biases.

CERES Comparison

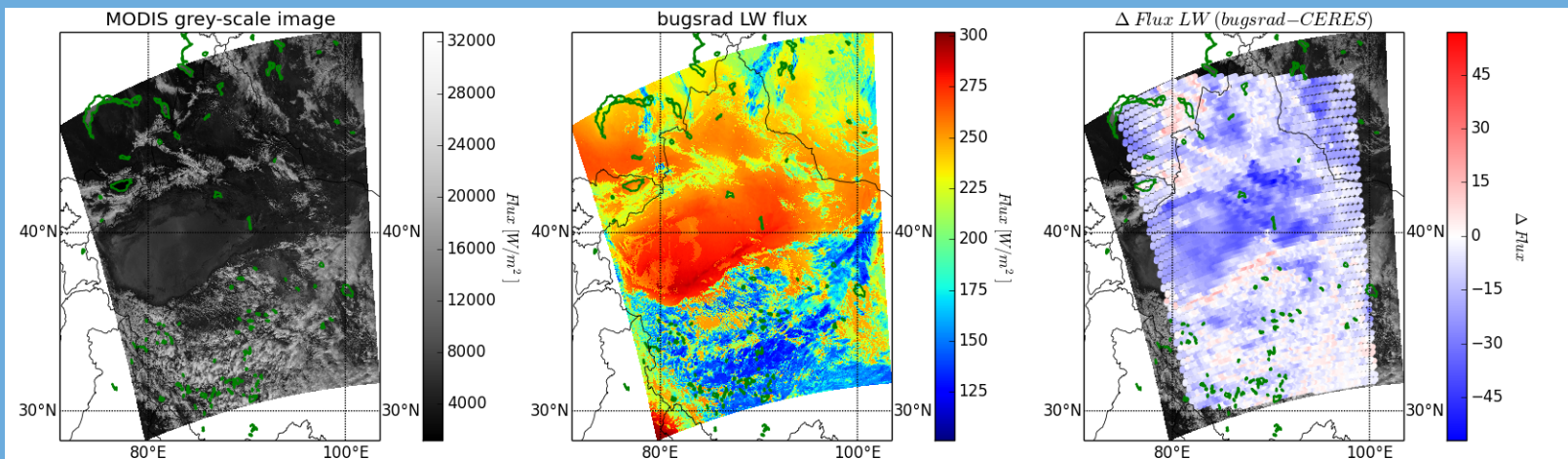
Central
Africa

Short
wave
Fluxes



Taklam
aken
Desert

Long
wave
Fluxes

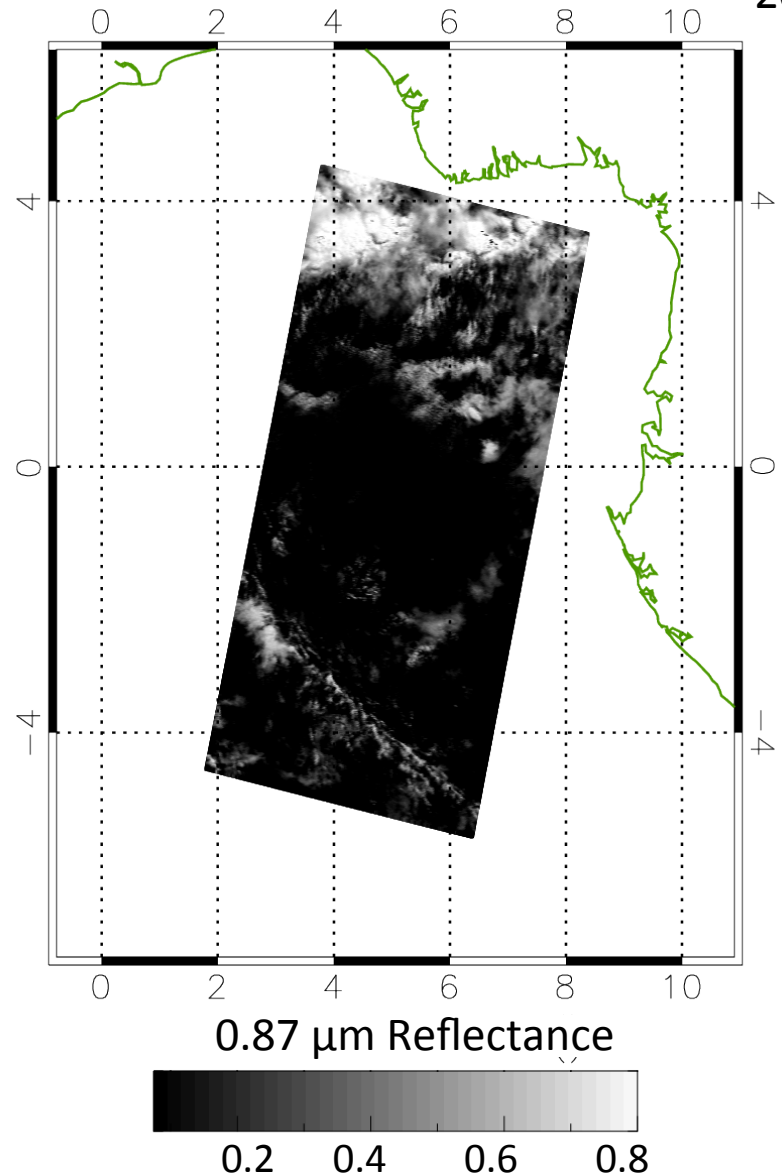


Areas of Improvement

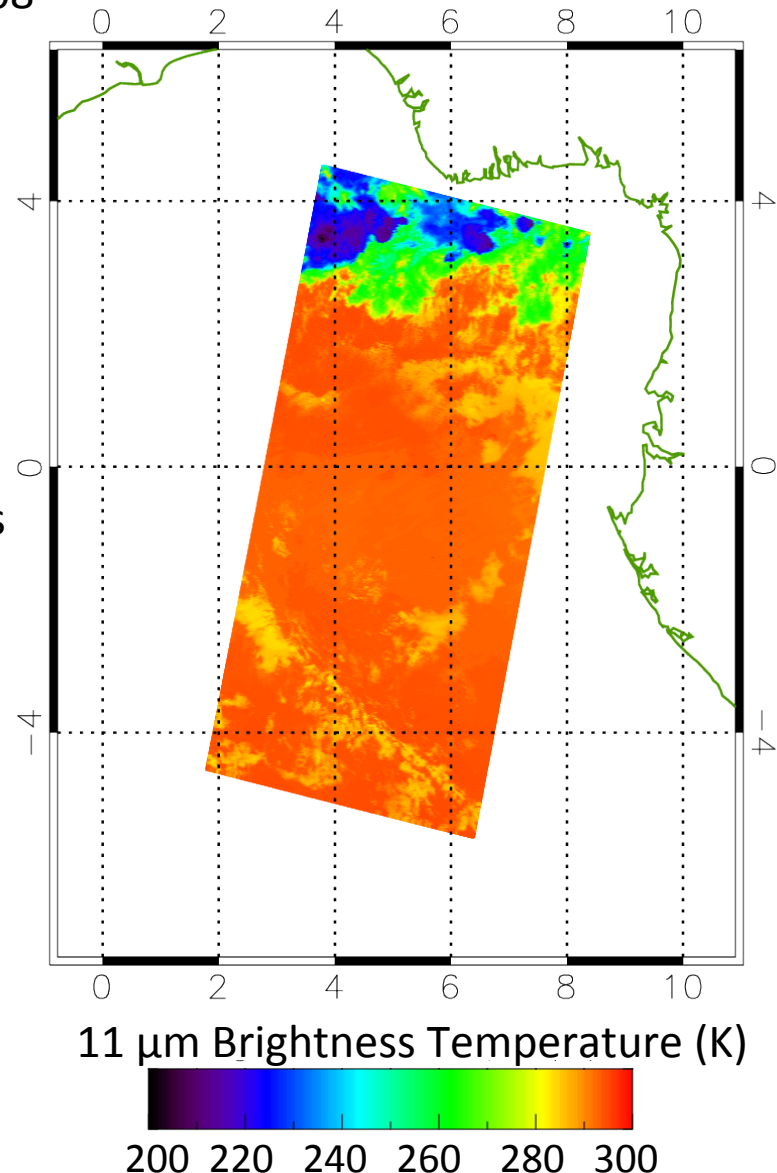
- Negative shortwave bias retrieved for ice clouds. Test LUTs for Baum and Bauran.
- Negative longwave bias over clear-sky desert regions → use LST retrieval instead of ECMWF.

GERB Comparison

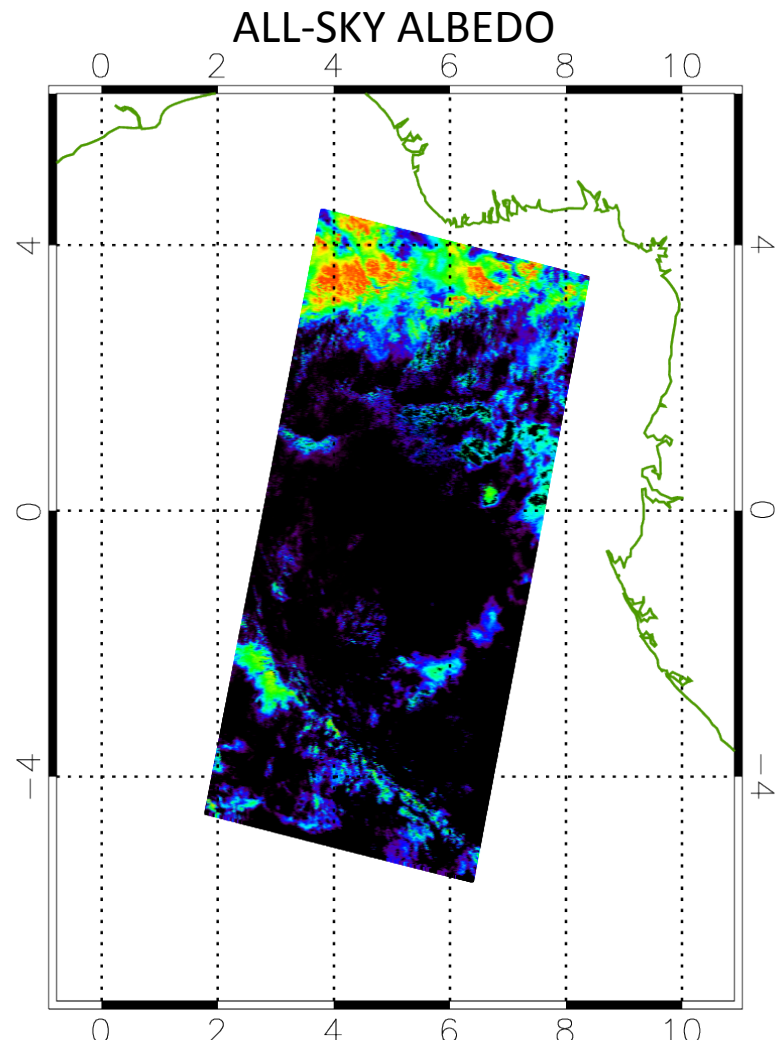
20th June 2008



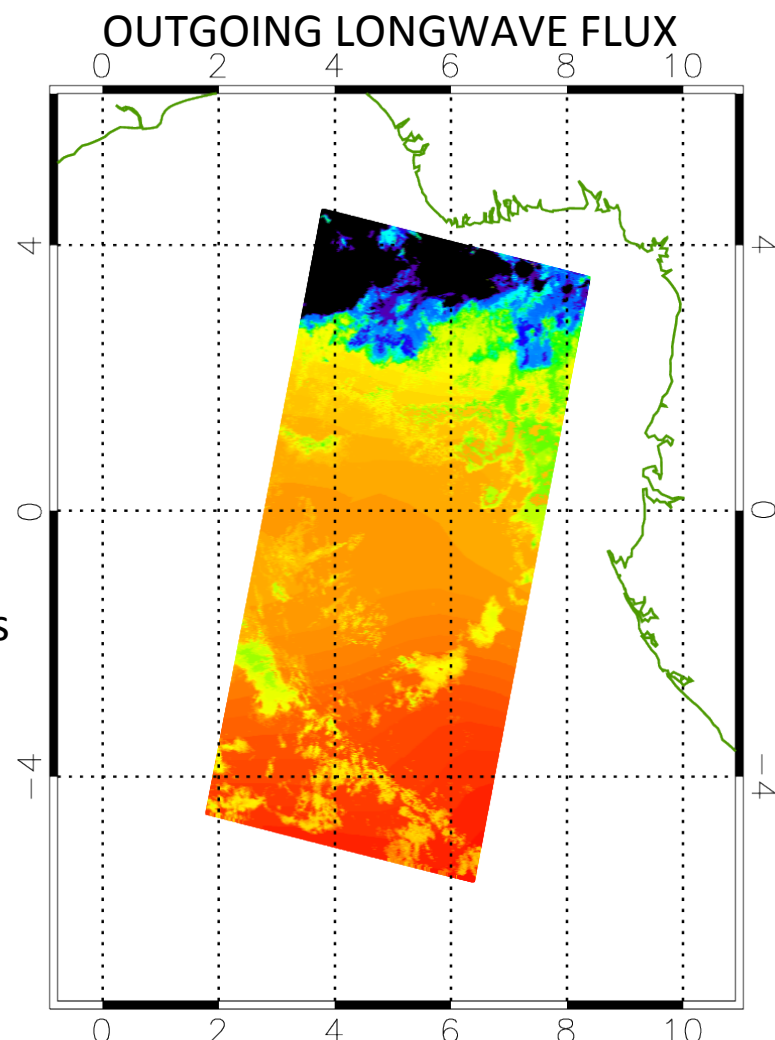
AATSR
1 km pixels



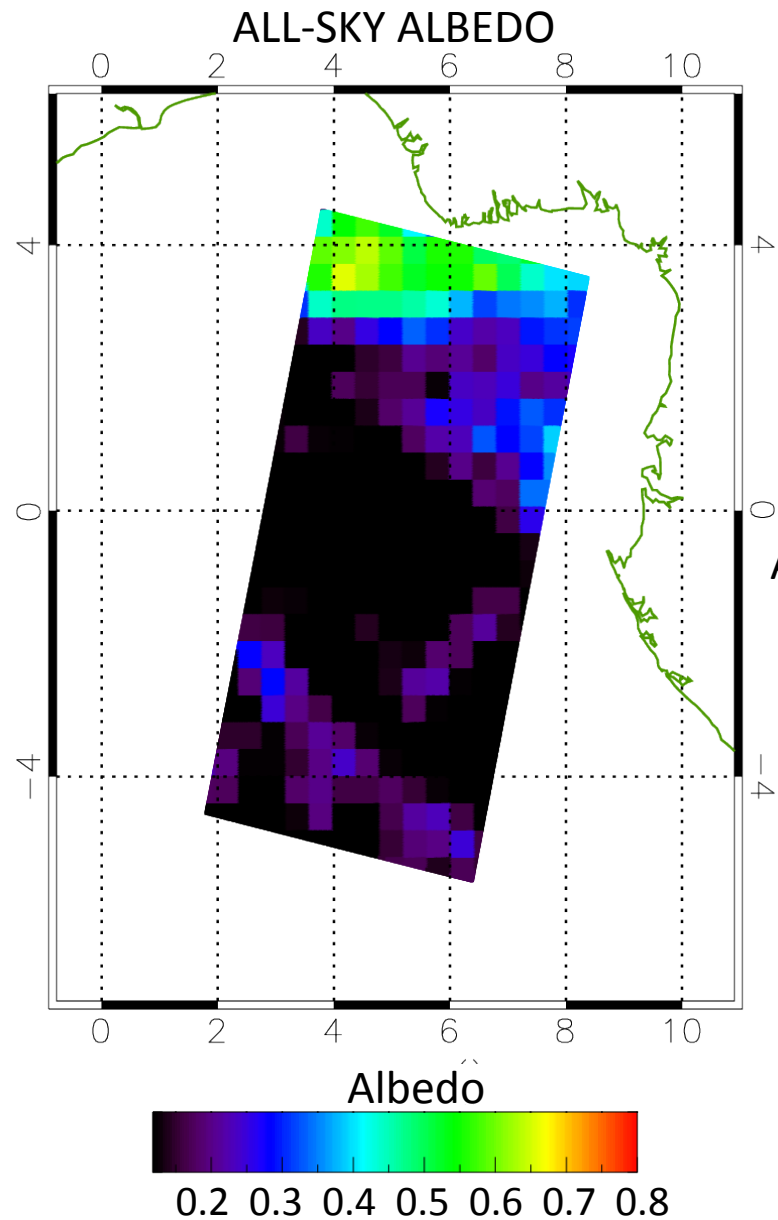
GERB Comparison



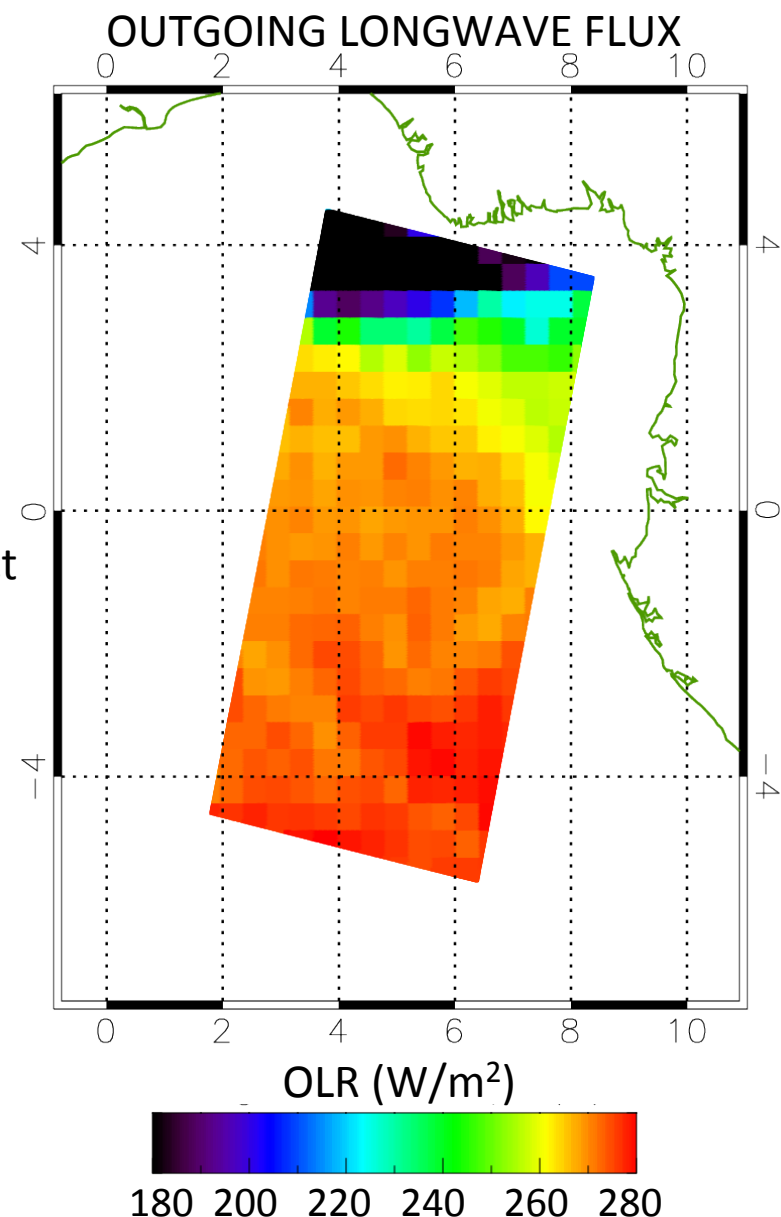
BUGSRAD
applied to
AATSR
1 km Pixels



GERB Comparison



GERB
ARG Product
44 x 39 km
Pixels



Cloud Radiative Effect

$$CRE = F_{CLR} - F_{OBS}$$

(1) Difference between clear-sky (F_{CLR}) and observed (F_{OBS}) flux.

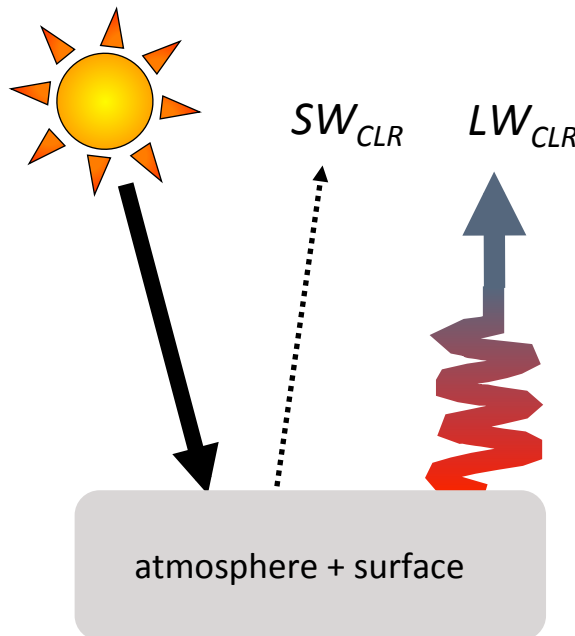
$$F_{OBS} = (1 - A_c) F_{CLR} + A_c F_{CLD}$$

(2) Observed flux: decomposed into clear and cloud fluxes.

$$CRE = A_c (F_{CLD} - F_{CLR})$$

(3) Combining (1) & (2)

F_{CLR} : Flux assuming no clouds

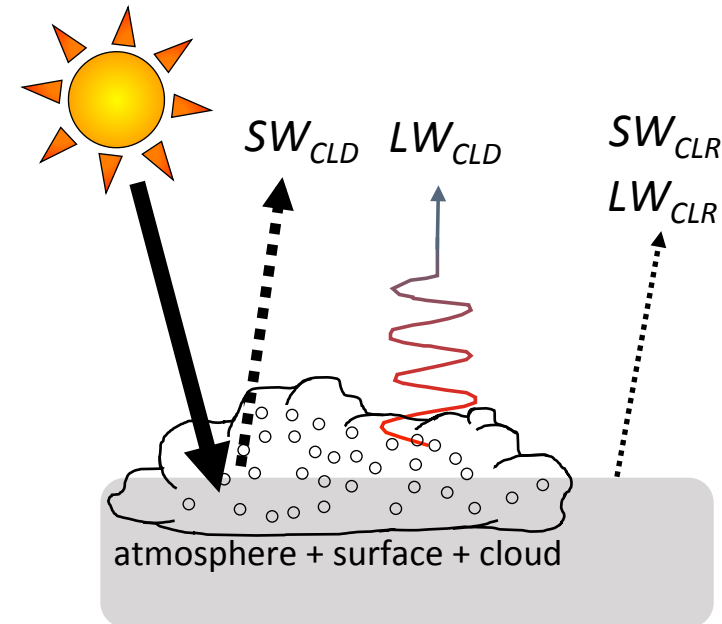


top of atmosphere

SW: shortwave
LW: longwave

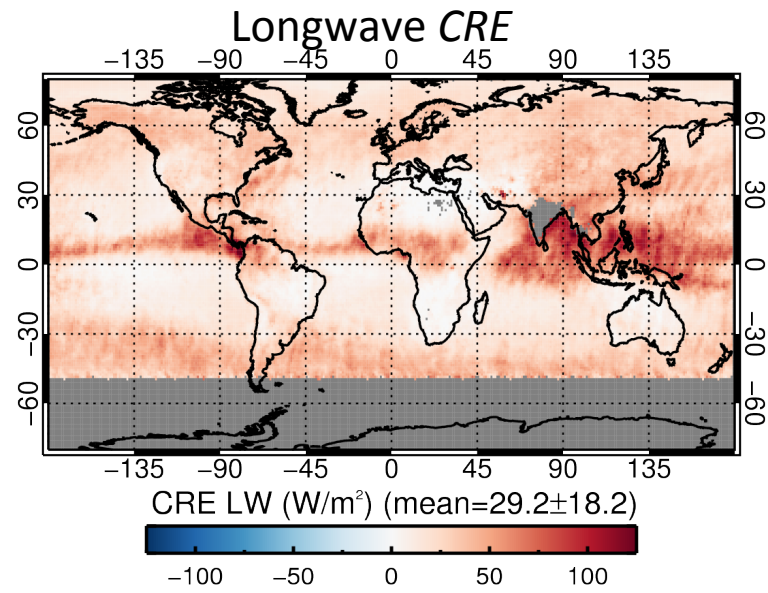
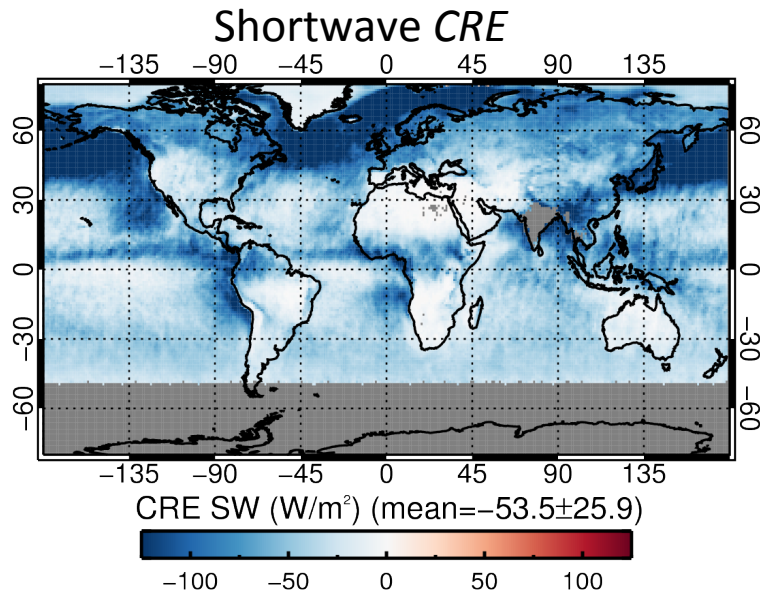
surface

F_{OBS} : Observed flux (clear + cld)



CRE : Effect of clouds on the reflected solar and emitted flux relative to the clear-sky flux.

AATSR: Cloud Radiative Effect



$$\text{NET} = -24.7 \pm 2.5 \text{ W/m}^2$$

In agreement with CERES (Loeb et al., 2009)

Instrument: AATSR

Spatial resolution: 1-km then aggregated onto a $1^\circ \times 1^\circ$ grid

Period: 10-Year July average for AATSR mission

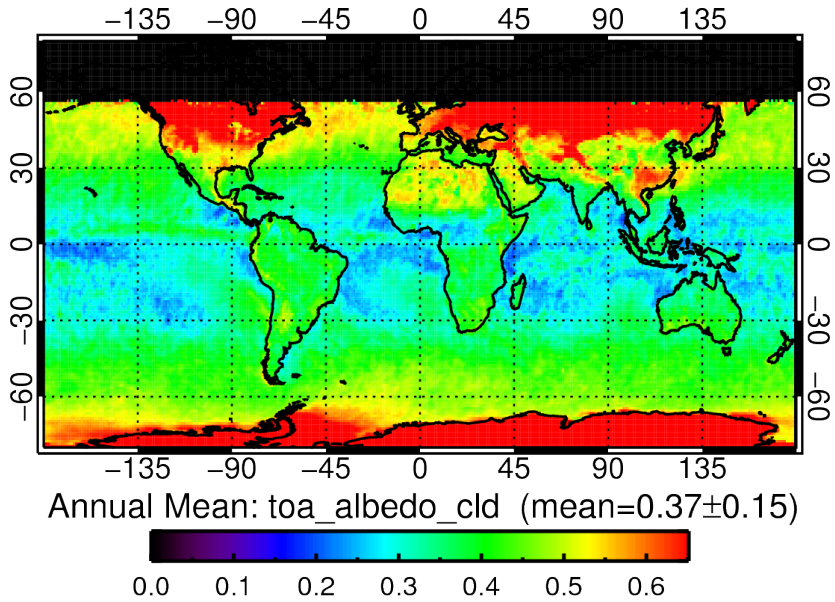
- Global mean values and standard deviations weighted by latitude are provided in brackets.
- *Instantaneous value* for shortwave *CRE* is converted to temporally interpolated fluxes based on monthly mean solar insolation (method described in Coakley et al., 1979, *JAS*, **36**).

Top of Atmosphere All-Sky Albedo

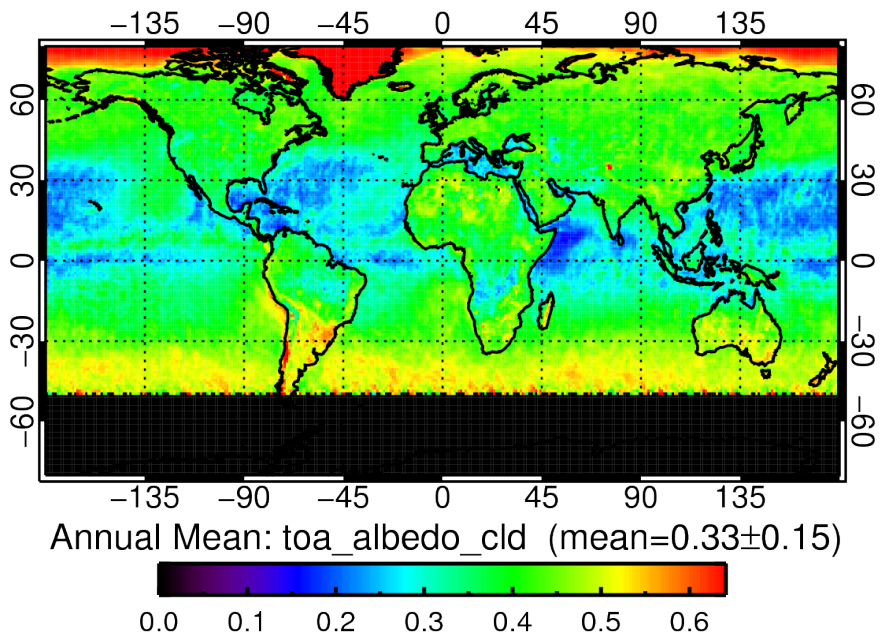
AATSR: 2002 – 2012 Monthly L3 Data

Top of atmosphere all-sky albedo

January long-term Mean



July long-term Mean

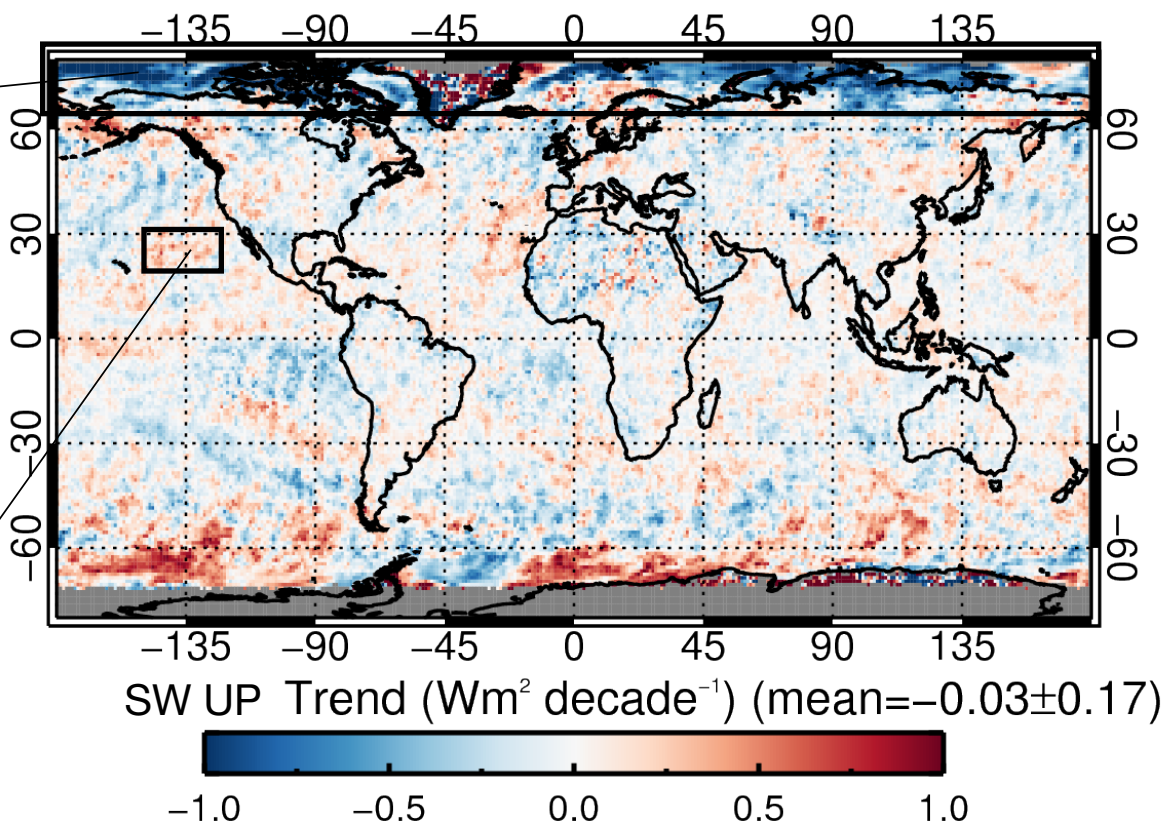
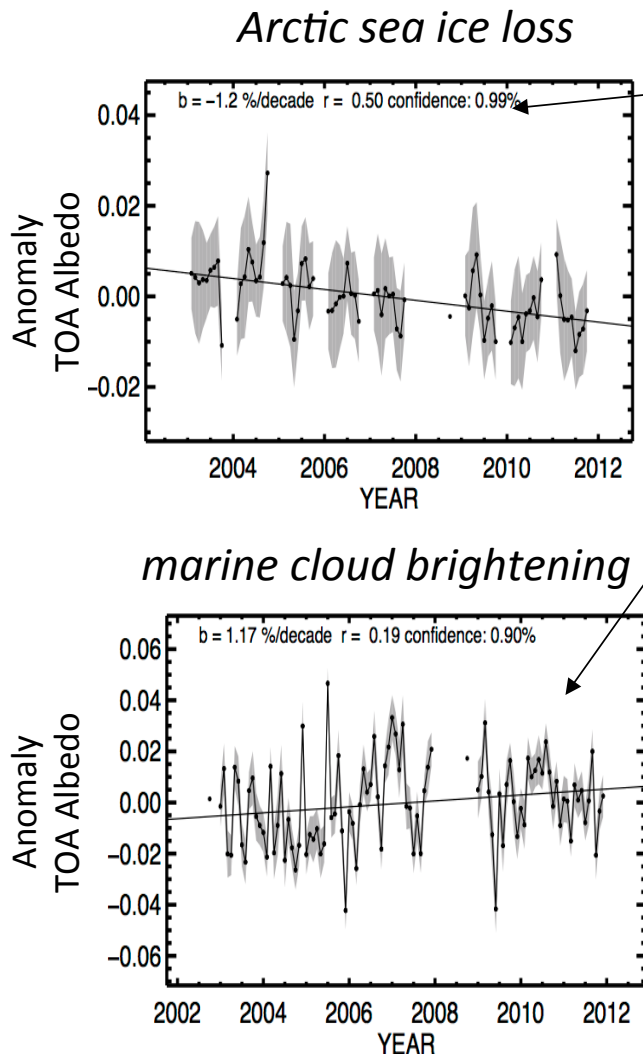


Features

- Sea Ice and Snow changes over Arctic, Antarctica, and Canada & Eurasia.
- Clouds: midlatitude storm tracks, ITCZ, and subtropical stratocumulus.

Trend: TOA All-Sky Reflected Solar Flux

AATSR: 2002 – 2012



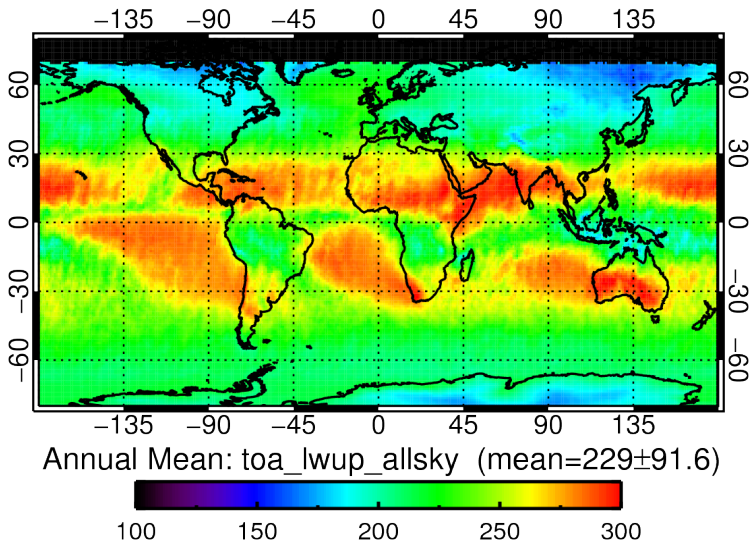
- Trends are consistent with CERES observations documented in (Hartmann and Ceppi, 2014, AMS)

Top of Atmosphere Emitted Longwave Flux

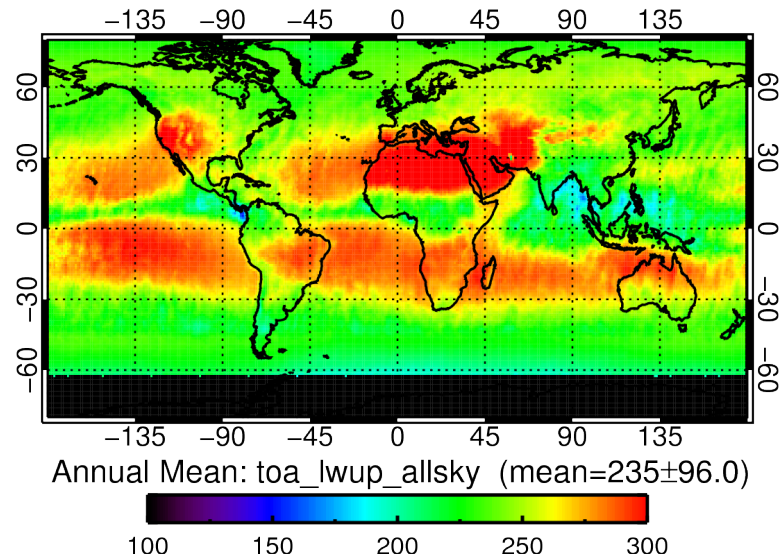
AATSR: 2002 – 2012 Monthly L3 Data

Top of atmosphere longwave emission

January long-term Mean



July long-term Mean

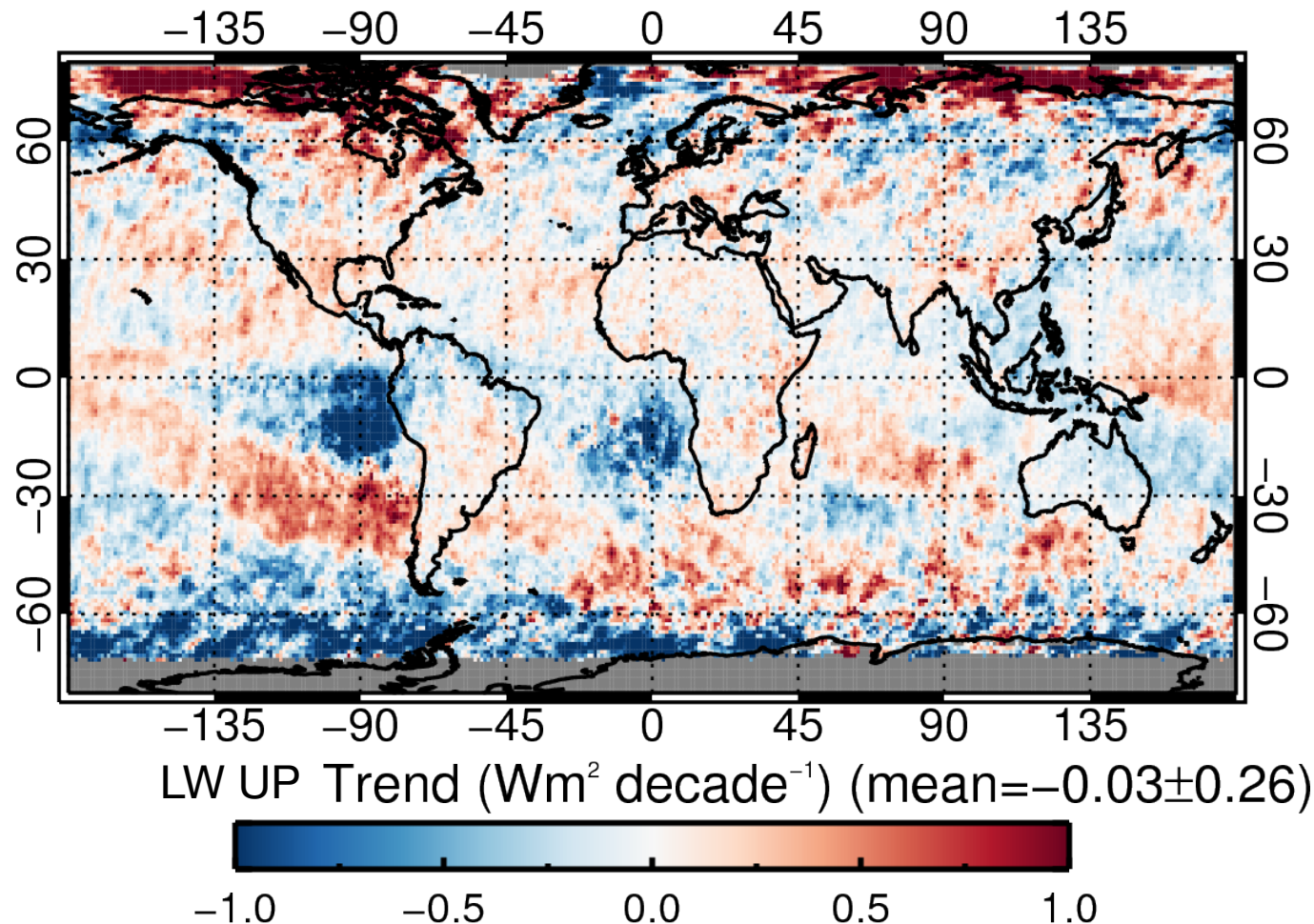


Features

- Large OLR over Subtropics and warm land areas (e.g., Saharan Desert)
- Clear northward shift in N.H. OLR between winter and summer.

Trend: TOA All-Sky Emitted Longwave Flux

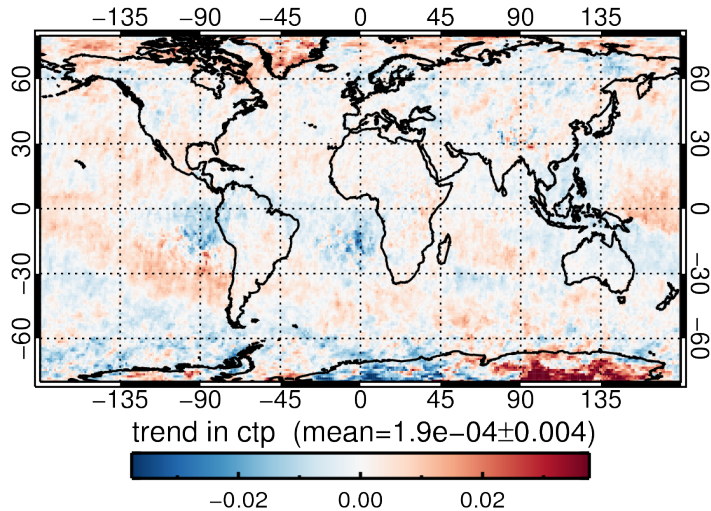
AATSR: 2002 – 2012 Monthly L3 Data



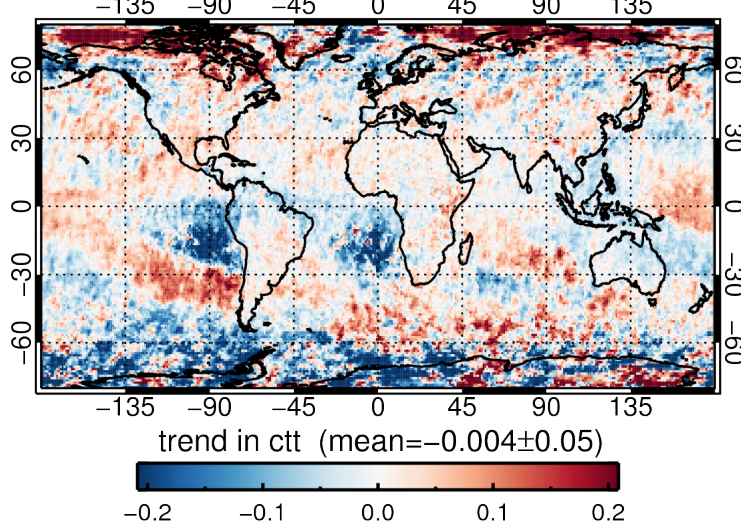
Trend: Cloud Properties

AATSR: 2002 – 2012 Monthly L3 Data

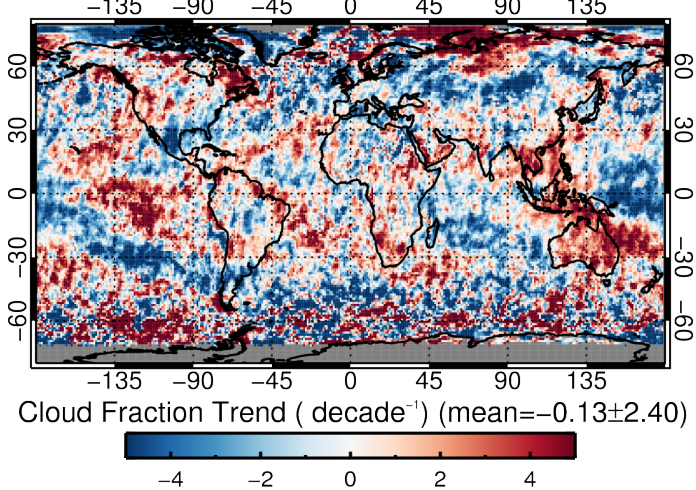
Cloud top pressure



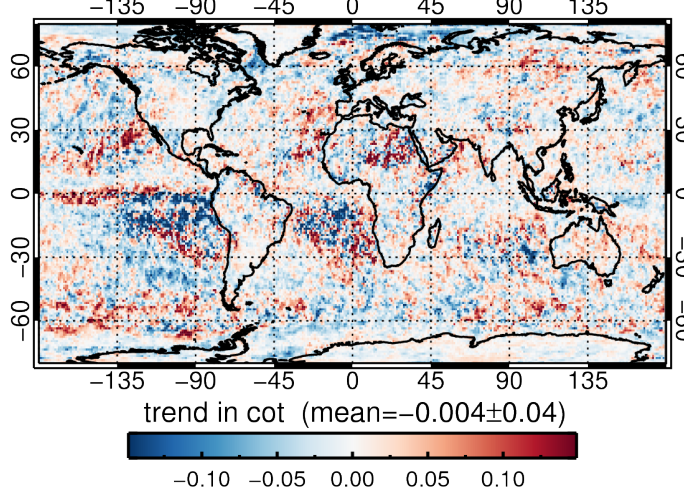
Cloud top temperature



Cloud Fraction



Cloud optical thickness



Summary

Main Findings

- New broadband radiation scheme can be applied to numerous satellite sensors at the pixel-scale resolution.
 - Trend analysis (AVHRR satellite series over 30 years of observations)
 - High spatial resolution application, e.g., ship tracks.
- Validation analysis shows strong agreement with high correlations and relative biases less than 10% relative error.
- AATSR trends show similar responses to CERES observations (Hartmann and Ceppi, 2014)

Further Work

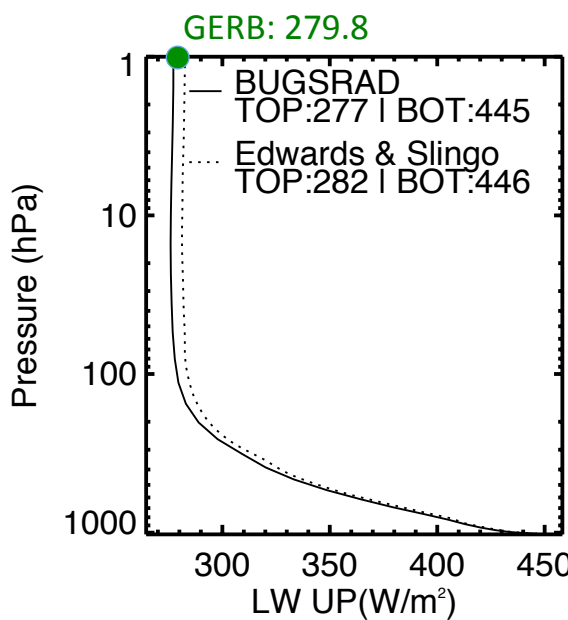
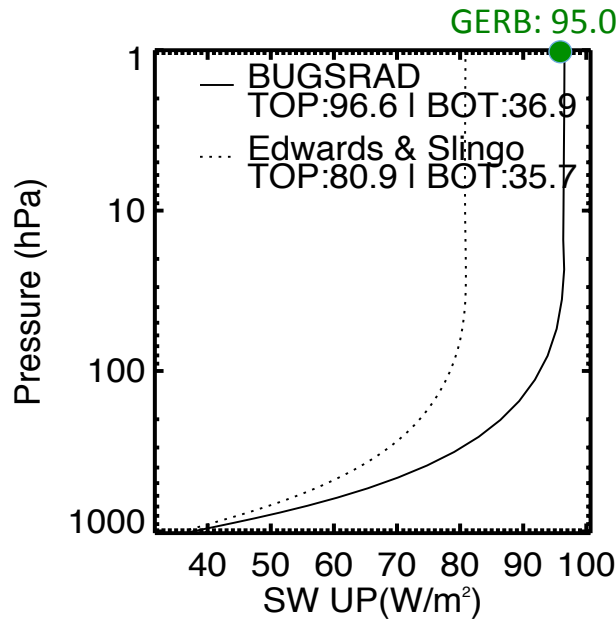
- Use overlap period between ATSR-2 (1995 – 2003) and AATSR (2002 – 2012) to constrain trend analysis for longer 17-year period.
- Improve ice cloud retrievals – comparison of look-up table properties.
- Apply data to the North Atlantic Climate System Integrated Study (ACESIS)

Acknowledgements

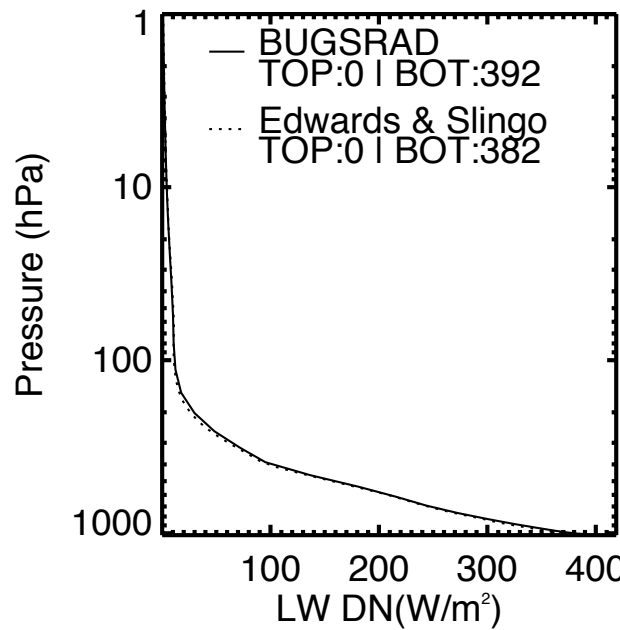
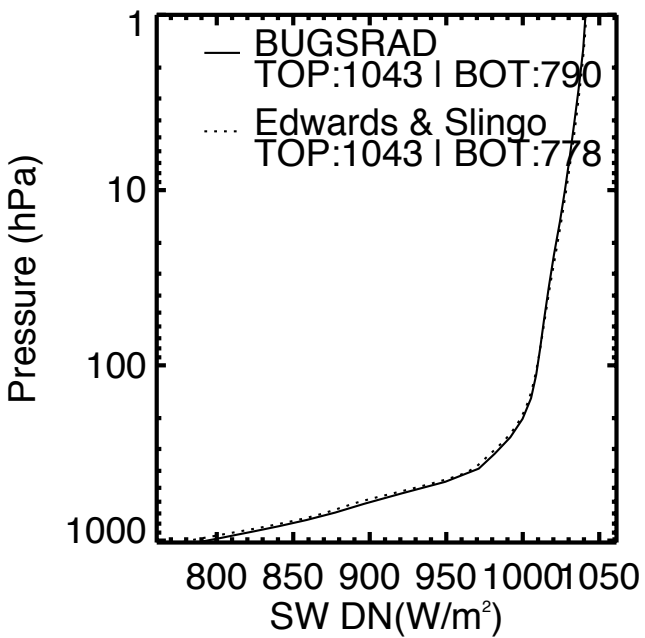
Support from the ESA-CCI programme

Production of data was carried out using CEDA JASMIN-CEMS.

Comparison with Edwards and Slingo



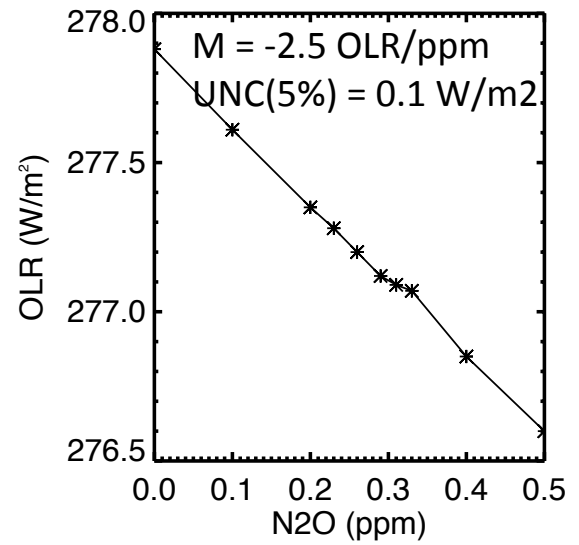
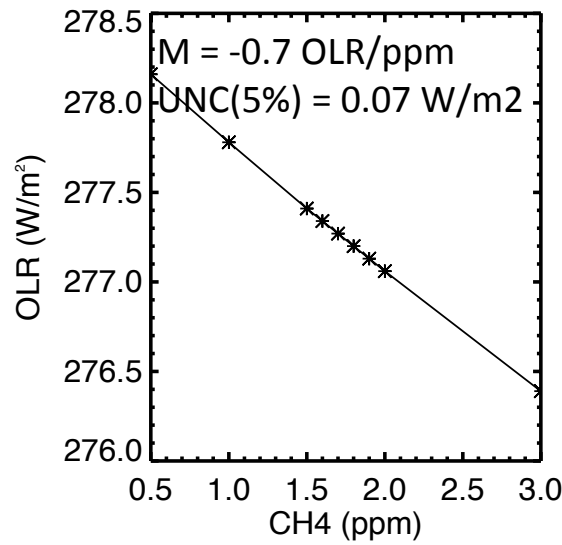
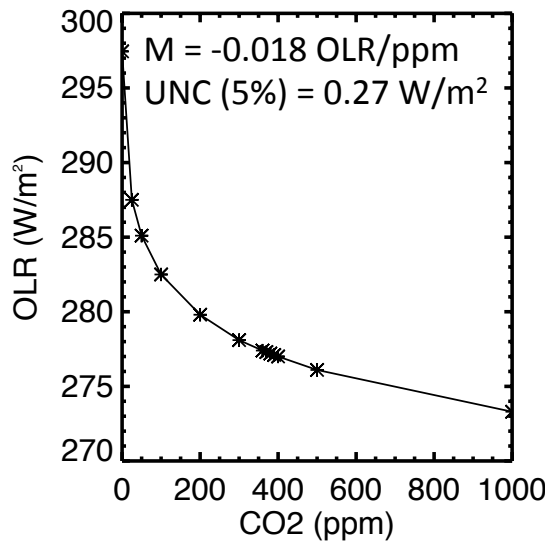
Clear-sky pixel over ocean coast of Africa
June 20th 2008
Latitude = -0.57°
Longitude = 5.74°



TOA fluxes

- Longwave differences between models are less than 5 W/m².
 - GERB result lies between models.
- Shortwave differences between models are less than 10 W/m².
 - BUGSrad closer agreement to GERB than Edwards Slingo.

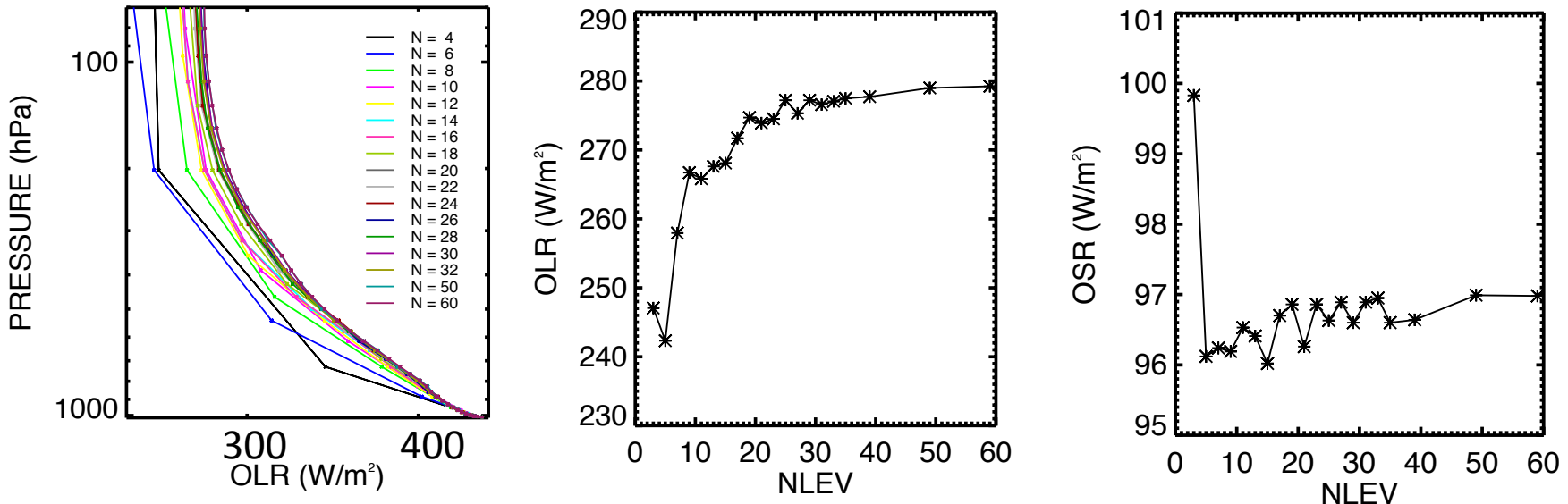
OLR Sensitivity to Gases



- Expected spatial variability (e.g., land VS ocean)
 - CO₂ ±15 ppm
 - CH₄ ±0.1 ppm
 - N₂O ±0.2 ppm

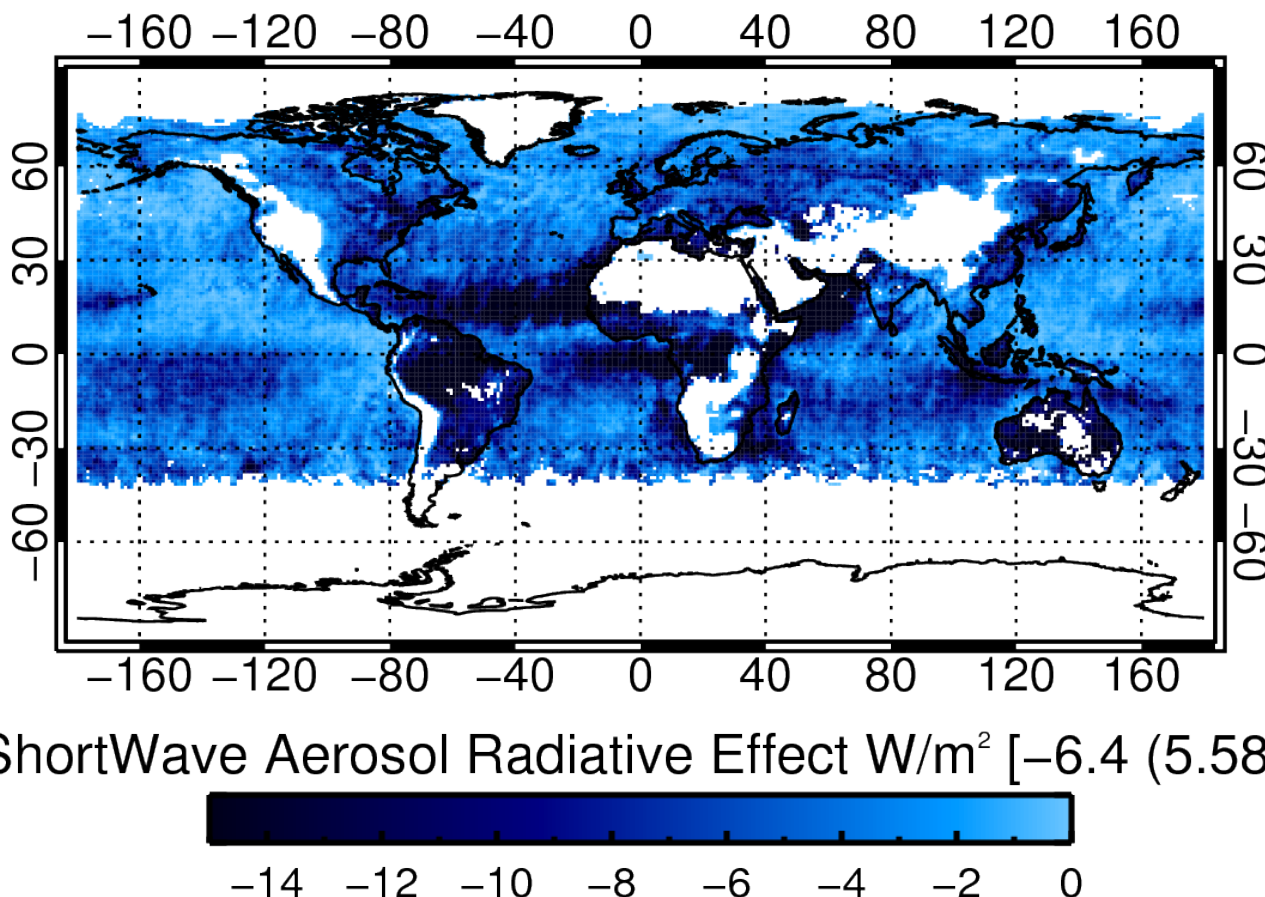
Maximum uncertainty from 5% variance: ±0.3 W/m²

Number of Vertical Levels



- Speed of algorithm *linearly* scales with # vertical levels in model.
 - Using 29 levels
- OLR at TOA is sensitivity to number of levels.
 - More levels increases OLR due to including more weight from lowest part of atmosphere.

Aerosol Radiative Effect



Aerosol direct effect: strong effects off coast of Africa and Hawaii.

Hartmann and Ceppi, 2014

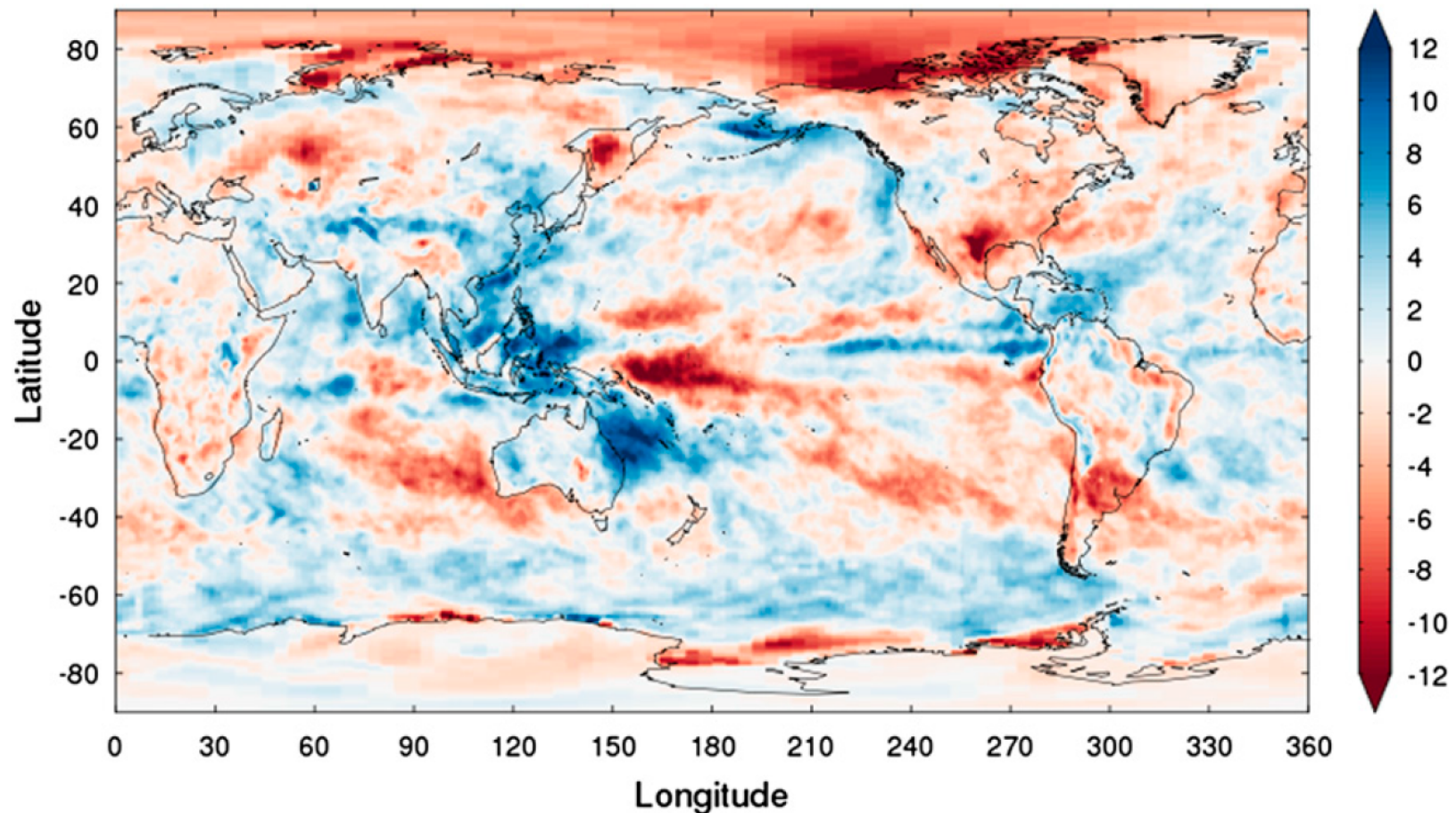


FIG. 3. Linear trend of CERES annual-mean reflected shortwave computed for each $1^\circ \times 1^\circ$ region of the globe ($\text{W m}^{-2} \text{decade}^{-1}$).

Energy Balanced Fluxes

- Instantaneous fluxes at 10:30 am equator crossing need to be normalised by monthly mean solar insolation.
- Incoming shortwave fluxes are energy balanced according to the mean solar insolation for each month.

$$\bar{F} = S_0 \left(\frac{r_0}{r} \right)^2 \int_{-H}^H \cos \theta_0 \frac{dh}{2\pi}$$

$$\cos H = - \tan \phi \tan \delta$$

Energy Balanced Flux

$$\frac{\bar{F}_{\downarrow SW\uparrow}}{\bar{F}_{\downarrow SW\uparrow}} = \frac{\bar{F}_{\downarrow SW\uparrow}}{\bar{F}_{\downarrow SW\uparrow} + \text{retrieved albedo}}$$

retrieved albedo

H: day length

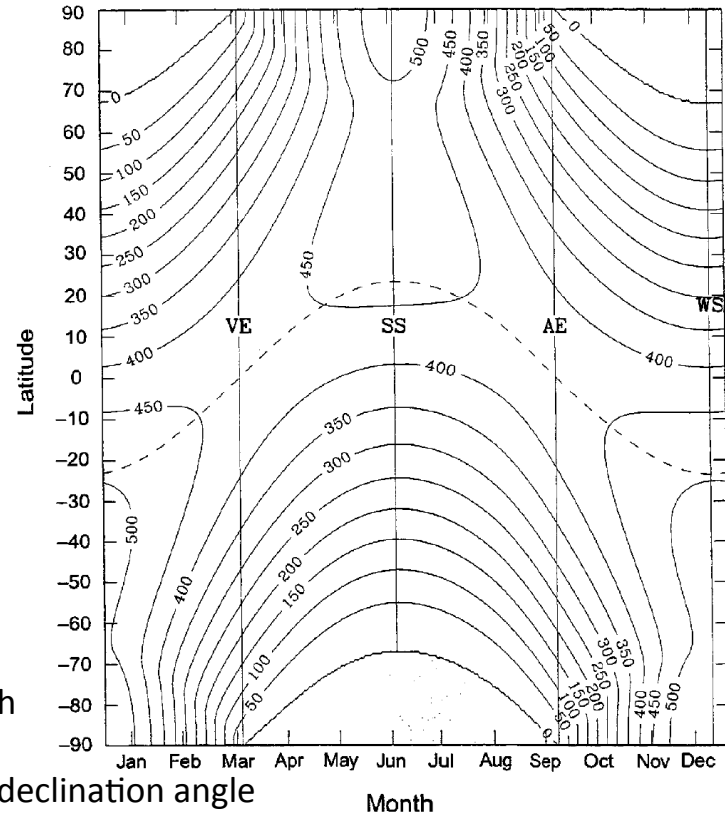
Phi: latitude

Delta: solar declination angle

So: solar constant: 1361 W/m²

(r₀/r)²: earth-sun distance

Theta₀: solar zenith angle



BUGSrad MODIS-TERRA fv2_0 ToA SWdn vs CERES - 2008

